Montclair State University

MONTCLAIR STATE UNIVERSITY

Montclair State University Digital Commons

Department of Earth and Environmental Studies Faculty Scholarship and Creative Works

Department of Earth and Environmental Studies

1997

Comparison of Source Rock Geochemistry of Selected Rocks from the Schei Point Group and Ringnes Formation, Sverdrup Basin, Arctic Canada

P. K. Mukhopadhyay
Atlantic Geoscience Centre

F. Goodarzi
ISPG (Geological Survey of Canada)

Michael A. Kruge
Montclair State University, krugem@mail.montclair.edu

M. H. Alimi
Global Geochemistry Corporation

Follow this and additional works at: https://digitalcommons.montclair.edu/earth-environ-studies-facpubs

 Part of the Geochemistry Commons, and the Stratigraphy Commons

MSU Digital Commons Citation

Mukhopadhyay, P. K.; Goodarzi, F.; Kruge, Michael A.; and Alimi, M. H., "Comparison of Source Rock Geochemistry of Selected Rocks from the Schei Point Group and Ringnes Formation, Sverdrup Basin, Arctic Canada" (1997). *Department of Earth and Environmental Studies Faculty Scholarship and Creative Works*. 636.
https://digitalcommons.montclair.edu/earth-environ-studies-facpubs/636

This Article is brought to you for free and open access by the Department of Earth and Environmental Studies at Montclair State University Digital Commons. It has been accepted for inclusion in Department of Earth and Environmental Studies Faculty Scholarship and Creative Works by an authorized administrator of Montclair State University Digital Commons. For more information, please contact digitalcommons@montclair.edu.

PREPRINT: Mukhopadhyay, P.K., Goodarzi, F., Kruge, M. A. and Alimi, M. H. (1997). Comparison of source rock geochemistry of selected rocks from the Schei Point group and Ringnes formation, Sverdrup basin, arctic Canada. *International Journal of Coal Geology* **34**:225-260. https://doi.org/10.1016/S0166-5162(97)00024-4

Comparison of Source Rock Geochemistry of Selected Rocks from the Schei Point Group and Ringnes Formation, Sverdrup Basin, Arctic Canada

P.K. Mukhopadhyay [a], F. Goodarzi [b], M.A. Kruge [c], M.H. Alimi [d]

[a] *Global Geoenergy Research Ltd., P.O. Box 9469, Station A, Halifax, NS , Canada B3K 5S3*
[b] *ISPG (Geological Survey of Canada), Calgary, Alta, Canada T2L 2A7*
[c] *Dept. of Geology, Southern Illinois University, Carbondale, IL 62901, USA*
[d] *Global Geochemistry Corporation, Canoga Park, CA, USA*

Abstract

Organic-rich from the Schei Point group (middle to late Triassic in age) and the Ringnes formation (late Jurassic) from the Sverdrup basin of the Canadian arctic archipelago have been geochemically evaluated for source rock characterization. Most samples from the Schei Point group are organic-rich (> 2% TOC) and are considered as immature to mature oil-prone source rocks [kerogen types I, I-II (IIA) and II (IIA)]. These kerogen types contain abundant AOM1, AOM2 and alginite (*Tasmanales, Nostocopsis, Leiosphaeridia*, acritarch and dinoflagellate) with variable amounts of vitrinite, inertinite and exinite. Samples from the Ringnes formation contain dominant vitrinite and inertinite with partially oxidized AOM2, alginite and exinite forming mostly immature to mature condensate- and gas-prone source rocks [kerogen type II- III (IIB), III and a few II (IIA)]. Schei Point samples contain higher bitumen extract, saturate hydrocarbons and saturate/aromatic ratio than the Ringnes samples. Triterpane and sterane (dominant C_{30}) distribution patterns and stable carbon isotope of bitumen and kerogen suggest that the analyzed samples from the Schei Point group are at the onset of oil generation and contain a mixture of sapropelic (algal) and minor terrestrial humic organic matter. Sterane carbon number distributions in the Ringnes formation also suggest a mixed algal and terrestrial organic matter type. There are some variations in hopane carbon number distributions, but these are apparently a function of thermal maturity rather than significant genetic differences among samples. Pyrolysis-gas chromatography/mass spectrometry of the two samples with similar maturity shows that the Schei Point sample generates three times more pyrolyzate than the Ringnes sample. Both samples have a dominant aliphatic character, although the Ringnes sample contains phenol and an aromaticity that is higher than that of the Schei Point sample.

Keywords: Arctic, organic facies, maturation, biomarkers, isotopes, pyrolysis-GC/MS

1. Introduction

During the past several years, significant oil, condensate and gas have been discovered in various reservoirs in the Arctic (Fig. lA). The Sverdrup basin of arctic Canada (approximately 100 km long and 300 km wide; Balkwill, 1978) contains a major sedimentary sequence of marine outer shelf, slope and basinal rocks (mainly argillaceous) of Carboniferous to early Tertiary age (Embry, 1984, 1991; Fig. lB). Two major rock sequences, the Schei Point group (middle to late Triassic-Anisian to Norian in age; Fig. lB) and the

Ringnes formation (late Jurassic: Oxfordian to Kimmeridgian in age; Fig. lB) have been studied in the past for their maturation, oil source rock potential and characterization of crude oil and gas in the basin (Baker et al., 1975; Snowdon and Roy, 1975; Henao-Londono, 1977; Powell, 1978; Monieret al., 1981; Goodarzi et al., 1987, 1989, 1992; Leith et al., 1992; Stewart et al., 1992; Brooks et al., 1992; Gentzis and Goodarzi, 1992a,b, 1993a,b; Gentzis et al., 1996). These studies have produced comprehensive knowledge on source rock and crude oil geochemistry for the basin and form a broad geochemical data base. Major organic-rich shales occur in the Schei Point group which has five transgressive and regressive cycles (Embry, 1989). The Ringnes formation has dark gray to black silty shale and siltstone that grades upward to the sandstone dominated Awaingak formation.

The present study is targeted to delineate the comparative spatial distribution of organic facies, maturation and hydrocarbon potential for various organic-rich rocks from the Schei Point group and Ringnes formation sampled from borehole sections at different locations (islands) of the Arctic (Fig. 2). This study examines source rock quality, thermal maturity and genetic interrelationships of the organic matter using organic petrography, selected parameters from the Rock-Eval pyrolysis, wet chemistry, biological marker geochemistry, stable carbon isotope and pyrolysis-gas chromatography /mass spectrometry (py-GC/MS).

2. Analytical methods

2.1. Samples

Nineteen samples of the Schei Point group (Eden Bay member, Cape Richards member, Murray harbour formation and Hoyle Bay formation) were selected for various analytical techniques. Sample information is shown in Table 1A with well names, depth and lithology. These samples were geochemically compared with seventeen selected samples of the Ringnes formation (Table 1B).

2.2. Methods

Three methods of sample preparation were used to study the organic facies and kerogen type by organic petrography: kerogen smear slide, whole rock polished pellet and kerogen polished pellet. The samples were studied by both incident and transmitted white light and by blue light excitation. The methods used for maceral composition in defining organic facies, depositional environment and hydrocarbon potential of a sedimentary rock requires precise examination of various maceral and submaceral components rather than only percentages of group macerals like vitrinite, inertinite and liptinite in a source rock (Stach et al., 1982; Mukhopadhyay et al., 1985; Teichmuller, 1986; Goodarzi and Stasiuk, 1987; Jones, 1987; Senftle et al., 1987, 1993 Mukhopadhyay, 1989; Mukhopadhyay and Wade, 1990; Stasiuk, 1991; Stasiuk et al., 1991; Whelan and Thompson-Rizer, 1993).

2.2.1. Rock-Eval pyrolysis

Rock-Eval pyrolysis was carried out on all those samples using the Rock-Eval II (Table 1A and B). For details of the Rock-Eval instrumentation and evaluation of the various parameters, see Espitalié et al. (1985). Only selected parameters (TOC, S1 and S2) in the Rock-Eval pyrolysis were listed in Table 1A and B. For T_{max} values of rocks of similar depths, the readers are requested to consult Brooks et al. (1992) and Stewart et al. (1992). A majority of the samples of the Schei Point group and the Ringnes formation for this study

were been taken from the similar depths and the same borehole as Brooks et al. (1992) and Stewart et al. (1992).

2.2.2. Bitumen extraction

Bitumen extraction was performed using approximately 30-50 g of coarsely crushed sample. The samples were powdered with the bitumen extracted by sonication in dichloromethane. Extractions were repeated using fresh solvent, until the solvent was clear. The extracts were taken nearly to dryness by rotary evaporation, then dried more thoroughly by exposure to a stream of nitrogen.

The extracts were fractionated by open column liquid chromatography, using activated silica gel, eluting with *n*-C_6H_{14}, *n*-C_6H_{14}:CH_2Cl_2 9:1, CH_2Cl_2 and CH_2Cl_2:CH_3OH 1:1, giving the saturate, aromatic and polar fractions respectively (Table 2).

2.2.3. Gas chromatography / mass spectrometry

For the gas chromatography/mass spectrometry analysis, the alkane fractions of the extract were analyzed by a Finnigan 9600 gas chromatograph (GC), coupled with a Finnigan 4000 mass spectrometer-data system (MS-DS). The GC was held initially to 100°C for 10 min, then raised to 220°C at 4°C/min and to 320°C at 2°C/min, where it was held for 25 min. A 60 M DB-1 capillary column was employed. The mass spectrometer was run in a selective ion monitoring (SIM) mode. Of about 20 fragment ions monitored by the SIM mode, the ionization fragments m/z 191 for triterpanes andm/z 217 for steranes are discussed in this study.

2.2.4. Stable carbon isotopes

The stable carbon isotopes of the saturate and aromatic fractions (from the bitumen extracts and kerogen fractions) were determined using a nuclide isotope mass spectrometer. All values reported here are relative to a PDB (Pee Dee belemnite) standard (Table 3). The stable carbon isotopes of the kerogen, alkane and aromatic fractions were determined by pyrolyzing the samples using cupric oxide. The resultant CO_2 was collected on a vacuum line in a pyrex breakseal tube. The $^{13}C/^{12}C$ ratio ($\delta^{13}C$) was determined against a standard on a dual collecting stable isotope ratio mass spectrometer.

2.2.5. Pyrolysis-gas chromatography / mass spectrometry

The pyrolysis-gas chromatography/mass spectrometry of two samples was carried out in the following manner: aliquots of powdered rock samples were subjected to pyrolysis-gas chromatography/mass spectrometry (py-GC /MS) using a CDS 120 Pyroprobe coupled to an HP 5890A GC and HP 5970B mass selective detector. The GC was equipped with a 50 m HP-1 column (0.2 mm i.d., 0.33 μm film thickness), initially held at 40°C for 5 min. then raised to 300°C at 5°/min then held for 20 min. The mass spectrometer scanned from 50 to 450 Da, with and ionizing voltage of 70 eV. The samples were first run in thermal extraction mode, in which the pyroprobe heated the sample at 310°C for 20 s, followed by a full GC run. Without removing the sample, it was then pyrolyzed at 610°C for 20 s and a full GC run was begun.

3. Results and discussion

3.1. Total organic carbon

All analyzed samples from the Schei Point group are organic-rich consisting of an above average total organic carbon (TOC) content of between 2.46% to 9.8% (Table 1A);

five samples have greater than 7% TOC. Total organic carbon content of samples from the Ringnes formation varies between 2.30% and 7.43%; three of them contain more than 6% TOC (Table 1B).

3.2. Organic facies and kerogen type using organic petrography

The maceral assemblage, grain size and their oxidation/fluorescence characteristics can unravel the history of organic matter accumulation, preservation, degradation by bacteria and eventually their hydrocarbon potential. This also demonstrates the change in maceral micro-texture due to the loss of organic carbon, hydrogen and oxygen by a sequence of advanced maturity.

The organic matter in sediments from both the Schei Point group and Ringnes formation has abundant amorphous components. The source rocks from the Schei Point group consists of mainly amorphous organic matter 1 and 2 (AOM1 and AOM2), whereas the organic-rich rocks from the Ringnes formation have partially oxidized AOM2. Amorphous organic matter 1 (AOM1) in the Schei Point group is formed mainly from the bacterial degradation of unicellular and filamentous algae (such as *Tasmanales, Nostocopsis, Leiosphaeorides*, etc. most of which occurs as telalginite; Fig. 3A, this article and Goodarzi et al., 1989; Stewart et al., 1992; Gentzis and Goodarzi, 1993a). AOM1 shows yellow to orange fluorescence, depending on the oxidation level, at low maturities (Fig. 3A and C). In normal reflected light, it shows an internal reflection (Fig. 4C). All mineral-bituminous groundmass that form from the mixture of AOM1 and minerals show a greenish yellow fluorescence. Amorphous organic matter 2 (AOM2) in both group of source rocks is derived from the bacterial degradation of dinoflagellates and acritarchs (Mukhopadhyay et al., 1985; Mukhopadhyay, 1989); bacterial lipids are usually incorporated within the amorphous organic matter 2. AOM2 has a brown to orange-brown fluorescence (Fig. 3D) and is often associated with lamalginite (Fig. 3D). In some source rocks, AOM2 is formed by the bacterial degradation of exinites (especially cutinite and suberinite; Mukhopadhyay and Wade, 1990). Under normal reflected light, unoxidized AOM2 appears as dark granular clustered bodies (Fig. 4A). Oxidized AOM2 shows various shades of white and light gray color (Fig. 4B). Under advanced maturation, AOM2 is converted to micrinite and alginite or exinite to rank-inertinite (Fig. 4D). The main criteria for the identification of AOM1 and AOM2 are their fluorescence characteristics at low maturities and their morphology as seen under transmitted light using smear slides (Mukhopadhyay et al., 1985; Mukhopadhyay, 1989; Mukhopadhyay and Wade, 1990). The macerals AOM1 and AOM2 are equivalents of bituminite or sapropelinite or amorphinite (Teichmuller and Ottenjann, 1977; Van Gijzel, 1981; Mukhopadhyay et al., 1985; Senftle et al., 1987; Mukhopadhyay, 1989; Mukhopadhyay and Wade, 1990). On the other hand, amorphous organic matter 3 (AOM3) is a degradation product of humic substances and some exinites (especially sporinite; Mukhopadhyay et al., 1985; Mukhopadhyay, 1989).

3.2.1. Schei point group

The analyzed samples from the Schei Point group contain abundant AOM1 and AOM2 with mixtures of telalginite and fresh or partially degraded dinoflagellates and acritarchs (occurring mostly as lamalginite; Fig. 3A, B and D, this paper; Stewart et al., 1992). Some samples contain more than 10% vitrinite [samples 94 (27), 133 (23) and 163 (19); Table 1A]. None of these rocks display any major oxidation effect on AOM1 and AOM2. Samples (20) 18, (44) 11, (60) 17, (72) 10 and (73) 1 contain *Tasmanales*, *Nostocopsis* and *Leiosphaerides* algae like other Schei Point source rocks as indicated by Goodarzi et al. (1989). Some samples contain *Botryococcus* algae suggesting a possible

lacustrine algal input. Vitrinite and inertinite are the major terrestrial macerals (Fig. 4C and D). With a few exceptions (94-27; 163-19), exinite is virtually absent in most samples. Most samples contain mainly fine-grained solid bitumen (yellow fluorescence) and oil droplets within AOM1 and AOM2.

The admixture of terrestrial macerals (vitrinite and inertinite) with AOM1, AOM2 and alginite (Fig. 4C) in most samples from this group indicates the following depositional environment of these rocks: (a) a possible open ocean anoxia on a carbonate platform, (b) a shallow marine environment (subtidal zone) with high organic productivity and periodic terrestrial input, (c) lacustrine anoxic environment in a lower delta plain. The nature of alginite and the abundance of AOM1 and AOM2 suggest that the probable depositional regime fluctuates between environment types (b) and (c).

Based on organic facies, grain size of the macerals (within the whole rock plug) and oxidation/fluorescence characteristics, the following conclusions were made: (a) Most samples are kerogen type I-IIA and IIA (II of Tissot and Welte, 1984); sample 60 (17) is of kerogen type I; all analyzed samples are considered as major liquid hydrocarbon source rocks. None of these rocks could be classified as kerogen type III or IV. (b) The depositional environment was anoxic to dysoxic and had a fair amount of terrestrial organic matter input.

3.2.2. Ringnes formation

Most of the samples contain abundant terrestrial organic matter (vitrinite, inertinite, exinite; Fig. 4A). In most cases, AOM2 is oxidized, hydrogen-depleted and has lost its fluorescence thus forming an amorphous maceral with micrinite similar to AOM3 (Fig. 4B; Mukhopadhyay et al., 1985; Mukhopadhyay, 1989; Mukhopadhyay and Wade, 1990). Some alginite (both lam- and telalginite) were also recorded in the Ringnes formation samples: sample 45 (6) contains some *Tasmanites* algae; samples 45 (6), 110 (24) and 139 (18) contain abundant lamalginite of unknown affinity, some of which are marine dinoflagellates. Samples 118 (22) and 161 (21) contain abundant yellow to brown fluorescent AOM2. A large percentage of alginite (both tel- and lam-) shows brownish fluorescence and is partially oxidized resulting in the formation of micrinite; most framboidal pyrite is also oxidized similar to that described in Mukhopadhyay and Wade (1990). Secondary liptinites (solid bitumen and oil droplets) are present in some source rocks usually within the AOM1 and AOM2 [example: sample 139 (18)].

The organic facies, grain size distribution of macerals and oxidation/fluorescence characteristics indicate that: (a) These rocks were formed in a dysoxic to oxic depositional environment as suggested by the presence of orange to red fluorescent AOM , alginite and exinite and oxidation of framboidal pyrite. However, the abundance of AOM2 and framboidal pyrite and its association with the fine grained clastics suggest an abundance of bacterial activity. (b) Except for two samples [41 (32), 55 (8)], all other samples are considered as kerogen type II- III or IIB (II-III of Tissot and Welte, 1984) which would generate mainly condensate and gas with minor crude oil (Mukhopadhyay and Wade, 1990; Mukhopadhyay et al., 1995). All mature and overmature kerogen type IIB source rocks were depleted in hydrocarbons changing their morphology in a similar fashion as kerogen type III source rock. (c) None of these samples were classified as oil-prone kerogen type I- IIA or II.

3.3. Rock-Eval pyrolysis, vitrinite reflectance and hydrocarbon potential

Of the Rock-Eval pyrolysis parameters, the hydrogen index (mg HC/g TOC) data of the Schei Point group show that most samples contain high values (> 450 mg HC/ g TOC) suggesting as type I or II kerogens, which has some algal affinity (Table 1A). The Rock-Eval pyrolysis data presented by Leith et al. (1992) from various other wells and the data from

Brooks et al. (1992) correlate with the hydrogen index data and the interpretation on source rocks based on organic petrography for this work.

The hydrogen index values of the Ringnes formation samples varied between 2 to 335 mg HC/ g TOC and was much lower compared to the Schei Point group samples (Table 1B). Stewart et al. (1992) included a modified van Krevelen diagram (hydrogen index versus oxygen index) which revealed that most samples lie within the kerogen type II and III or III maturation path (Tissot and Welte, 1984).

The vitrinite reflectance data of the analyzed Schei Point samples suggest that most samples lie within the immature to mature zones (0.4 to 0.7% R_o; Table 1A). Considering the abundance of AOM1 and AOM2, two samples [83(20), 133(23)] have advanced maturity sufficient for hydrocarbon generation and expulsion. Organic facies data (i.e. presence of abundant micrinite within AOM1 and AOM2) suggest that those samples are depleted in hydrocarbons. The samples from the Ringnes formation show a maturity of 0.45% [sample: 139 (18)] to 1.40% R [sample: 69 (31)]. However, similar to the Schei Point group, most samples lie within the immature to mature zone (0.44 to 0.75% R). According to an earlier report, most samples from the Ringnes formation have two distinct spore colorations suggesting mixing of autochthonous and allochthonous spores (Mukhopadhyay, 1993a). For details on the maturity with depth and the regional maturity of the Sverdrup basin, see Gentzis and Goodarzi (1992a,b, 1993a,b) and Gentzis et al. (1996).

Using a plot of vitrinite reflectance and hydrogen index, the comparable maturation paths of the Schei Point group and Ringnes formation samples have been illustrated (Fig. 5). Additional samples obtained for earlier reports were included in this plot (Mukhopadhyay, 1992a,b; Mukhopadhyay, 1993). Accordingly, most samples from the Schei Point group fall within the kerogen type I and IIA maturation path. On the contrary, samples from the Ringnes formation lie with kerogen type IIB and III.

Comparing organic facies, hydrogen index and maturity from this work and the Rock-Eval data from the earlier studies on similar samples from the same boreholes, the following observations can be drawn on the source rock potential of the samples (Brooks et al., 1992; Leith et al., 1992; Stewart et al., 1992; Mukhopadhyay, 1992a, 1993):

Schei Point group. (a) Rocks of the Cape Richards formation (deposited in a highly anoxic depositional regime) form the most prolific oil-prone kerogen type I or 1-IIA material while the Eden bay, Murray harbour and Hoyle Bay formations of this group contain multiple source rock types deposited in anoxic to dysoxic environments from variations in organic input and oxidation level (Mukhopadhyay, 1992a). (b) Multiple source rocks were present in the Schei Point group (Brooks et al., 1992; Leith et al., 1992; present work); a vast majority of samples are of kerogen type I, 1- IIA or IIA and can generate abundant liquid hydrocarbons; some of them are depleted at present in liquid hydrocarbons because of advanced maturity. Only a minor fraction of source rocks from the Schei Point group are considered as kerogen type IIB which mainly generates condensate and gas (Mukhopadhyay, 1992a,b; Brooks et al., 1992). (c) Considering the abundance of so many oil-prone source rocks within the Schei Point group, it is likely that a majority of crude oils in the western Arctic Islands were derived from the source rocks of the Schei Point group.

Ringnes formation. (a) Organic matter is composed of mixed terrestrial and algal-derived material deposited in a shallow marine to deltaic environment; lipid-rich macerals are partially oxidized forming hydrogen-depleted source rock. (b) Multiple source rocks are present, most of which can generate condensate and gas (kerogen type IIB and III). This is contrast to the presence of vast majority of oil-prone source rocks within the Schei Point group. Considering the presence of abundant kerogen type IIB source rock and the slightly higher maturity of the region, the presence of condensate and gas reservoir either in the

Ringnes formation or nearby reservoir rock stratigraphically higher to the Ringnes formation (e.g. Awingak formation) is anticipated.

3.4. Bitumen extraction and liquid chromatography

Selected Schei Point group source rocks have total bitumen extracts ranging from 9.9 to 63.3 mg HC/g TOC with sample 20 (18) giving the lowest amount and sample 52 (12) giving the highest bitumen content (Table 2). Those values are typical of immature to marginally mature (early mature) source rocks with good hydrocarbon source potential. Samples 133 (23), 52 (12) and 64 (29), which display the highest bitumen values (> 30 mg/g Corg, Table 2), appear to be influenced both by the organic facies and maturity. Those samples are kerogen type 1-II or II and contain abundant amorphous liptinite (AOM1 and AOM2).

The fractionation data show that the extracts contain 40.4% to 83% hydrocarbons (total of saturates and aromatics), with saturates (aliphatics), constituting 58.4% to 68.7% of total hydrocarbons (Table 2). In most samples, the saturate/aromatic ratios are above 2 and saturate/polar ratios are above 1. The high saturate/aromatic ratio in some source rocks from the Schei Point group may suggest that the vitrinite reflectance has been suppressed due to the presence of abundant bitumen content. The relatively low extract yields with higher polar compounds in some samples indicate that those samples are at an immature to marginally mature stage.

Within the samples from the Ringnes formation, yields of extractable organic matter (EOM) varied from 9.0 to 46.0 mg HC/g TOC (Table 2). EOM contents do not increase with increasing total organic carbon (TOC) content. However, two samples 35 (12) and 55 (8) have > 40 mg HC/g TOC. Most of the variation in the liquid chromatographic results are in the yields of saturates, which run from 5% to 52% (mean = 32%, standard deviation = 11) of the total extracts for the Ringnes formation.

Fig. 6 shows the comparable plot of TOC and bitumen extract for both the Schei Point and Ringnes samples. Fig. 7 plots the extract bulk composition on a ternary diagram. It is apparent that the samples from both stratigraphic units show considerable variability. However, it is clear that, overall, the Schei Point group are enriched in saturates, while Ringnes fm. samples have more NSO compounds. This suggests that the Ringnes formation has less algal affinity and was probably deposited under partially oxidizing conditions.

3.5. Normal and cycloalkane ratios and CPI

Table 3 illustrates the C_{15}+ isoprenoid/normal alkane ratios (i.e. pristane/phytane, pristane/*n*-C_{17} and phytane/*n*-C_{18}) and the carbon preference index (CPI) which are derived from gas chromatography/mass spectrometry (m/z 99 mass fragmentograms). Based on the alkane distribution patterns of the Schei Point group samples, they are thermally immature (odd-even dominance) to moderately mature (CPI approaches 1), containing hydrocarbons predominantly derived from sapropelic (algal) kerogen mixed with a small proportion of terrigenous plant material. In selected source rock samples from the Ringnes formation, considerable variation exists in their normal alkane distribution, particularly in the extent of odd/even carbon number preference in the C_{21}-C_{33} range. The odd preference in the C_{23} to C_{33} range is particularly strong for samples 161 (20), 161 (21), 118 (22) and 110 (24), with CPI values of 1.72 to 2.14. The odd preference is much weaker in samples 45 (7), 55 (8), 35 (12) and 35 (13) (CPI:1.17 to 1.30). In general, most of the samples appear to be thermally immature and to be derived from organic matter that has a significant terrestrial component, mixed with material of algal origin. Samples 45 (7), 55 (8) and 35 (12) are apparently derived

from organic matter similar to the others, but are more mature. This conclusion is supported by the higher concentrations of saturated hydrocarbons found in those samples (Table 3).

Pristane/phytane ratios are relatively high in all samples (1.24-2.93, Table 3), consistent with the presence of a large terrestrial organic matter component. However, the ratio is not as high as those typically seen in samples containing only terrestrial material (pristane/phytane > 4 or 5), indicating that the samples contain organic matter of mixed origin.

Fig. 8 represents a plot of pristane/*n*-C_{17} and phytane/*n*-C_{18}. On such a diagram, samples of similar origin tend to plot linearly along a ray whose angle with the abscissa is a function of the organic matter type. A low angle is characteristic of algal organic matter, whereas an angle above 70° is typical of terrestrial origin (Connan and Cassou, 1980). In general, the higher the pristane/phytane ratio, the greater the angle. The isoprenoid/*n*-alkane ratios are also, in part, a function of maturity with more mature samples tending to plot closer to the origin. The dominant sapropelic origin of the organic matter present in samples of the Schei Point group and dominant mixed to terrestrial organic matter in the Ringnes formation is evident in Fig. 8 (Connan and Cassou, 1980). Among Schei Point samples, 29 (25), 133 (23) and 97 (5) show a slightly different trend than samples 44 (11) and 60 (17). These differences are probably due to their level of maturity [for sample 133 (23)] or to the differences in their depositional environment or both (for sample [29 (25)]. Two Ringnes formation samples, 110 (24) and 161 (20), apparently of low maturity, have the highest isoprenoid/*n*-alkane ratios. They fall into the algal field in Fig. 8, which is consistent with the petrographic data (Table lB).

3.6. Saturate biomarkers

3.6.1. Pentacyclic and tricyclic triterpanes

The hopanes are the predominant compounds shown in the m/z 191 mass chromatogram of Schei Point group sample 60 (17) (Fig. 9A). The tricyclic terpanes are of secondary importance. The most notable features of this sample are the presence of C_{27} 17β hopane and C_{29}-C_{33} 17β,21β hopanes, abundant moretanes and a strong predominance of 22R isomers over the 22S among the C_{31}-C_{35} 17α,21β hopanes. These characteristics indicate a low level of thermal maturity.

Schei Point group sample 133 (23), shown in Fig. 9B, presents a rather different picture, with a significantly greater contribution of tricyclic terpanes, including long chain homologues (up to at least C_{34}). The 17β and 17β,21β hopanes are not detectable, the concentrations of the 22S extended hopane isomers are greater than that of the 22R, the moretanes are less abundant, all indicating a higher maturity (Seifert and Moldowan, 1980). The C_{29} 18α(H) hopane and C_{30} 17α(H) diahopane are important secondary components. These compounds appear to be thermally stable (Horstad et al., 1990; Fowler and Brooks, 1990) thus their abundance in Fig. 9B further supports the high maturity designation for sample 133 (23). They also appear to be characteristic of oils derived from source rocks containing active clays, deposited under environmental conditions ranging from dysoxic to anoxic (Moldowan et al., 1991).

It is noteworthy that the kerogens of the two Schei Point group samples discussed above are also petrographically distinct, with sample 60 (17) predominantly composed of AOM1, 133 (23) is mostly AOM2 (Table 1B). Thus the differences in their triterpane distributions are likely to be due to organic matter type, as well as thermal maturation, exemplifying the range of variability to be found among Schei Point group rocks.
In sample 161 (20) from the Ringnes formation, triterpanes are dominated by C_{27}-C_{32} hopanes (Fig. 10A). Tricyclic terpanes and longer chain hopanes are only minor components.

The C_{27} 17β(H) hopane and moretanes are relatively strong and 22R configuration is dominant among extended 17α,21β hopanes, although the situation is less extreme than was seen with sample 60 (17). The 17β,21β hopanes are not detected. These features indicate a low level of thermal maturity, but not as low as in the case of sample 60 (17).

Ringnes sample 45 (7) is similar overall to 161 (20) in its hopane carbon number distribution and lack of tricyclic terpanes. However, the lower abundance of C_{27} 17β(H) hopane and the moretanes, along with the predominance of the 22S isomers over 22R indicates a significantly higher maturity. A comparison of Figs. 9 and 10 indicates that the Schei Point group and Ringnes samples can be readily distinguished by their triterpane distributions, regardless of maturity level. The most striking differences are the greater relative abundances of tricyclic terpanes and C_{33}-C_{35} extended hopanes in the Schei Point group samples. This reflects the differences in their kerogen composition, with the Schei Point group samples having significantly less terrestrial organic matter than those of the Ringnes formation (Table 1A and B). These features should be exploited in oil-source rock correlation studies in this basin.

3.6.2. Steranes

The m/z 217 mass chromatogram of Schei Point group sample 60 (17) shows a predominance of C_{27} and C_{29} 5α,14α,17α(20R) steranes (Fig. 11A). The C_{28} $\alpha\alpha\alpha$(20R) sterane is also important. The 5β(H) steranes are present as secondary components. These characteristics are indicative of low thermal maturity, in accord with the hopane data. Rearranged steranes in this and other Schei Point group extracts suggest a marine depositional environment.

Schei Point group sample 133 (23) appears very different, having a predominance of 5α,14β,17β steranes and the 13β,17α diasteranes, in particular the C_{27} and C_{29} homologues in both cases. Short chain (C_{21} and C_{22}) steranes are also important. This indicates a higher level of thermal maturation, again in agreement with the triterpane data.

The representative Ringnes formation samples shown in Fig. 12 include low maturity sample 161 (20), with predominant $\alpha\alpha\alpha$(20R) steranes (especially C_{29}) and relatively strong 5β(H) steranes. Sample 45(7) is of higher maturity, as $\alpha\alpha\alpha$(20S) and $\alpha\beta\beta$ steranes are stronger. For both samples, the C_{27} and C_{29} $\beta\alpha$ diasteranes are prominent.

The samples can be conveniently compared on a ternary diagram showing the relative percentages of C_{27}, C_{28} and C_{29} $\alpha\alpha\alpha$20R steranes (Fig. 13; Table 6). A high proportion of C_{29} steranes is generally expected to occur in oils and source rock extracts derived from sediments containing mostly terrigenous (humic) organic matter (Huang and Meinschein, 1979). The Schei Point group samples plot closely together in Fig. 13, all showing nearly equal amounts of C_{27} and C_{29} homologues, but a deficiency in C_{28}. The Ringnes formation samples are all distinctly enriched in the C_{29} sterane and greater variability is observed. Organic matter type is evidently the major factor controlling the sterane carbon number distributions in these samples. As the ratio of alginite plus amorphous organic matter (AOM1 and AOM2) to vitrinite decreases, so does the ratio of C_{27} to C_{29} steranes (Fig. 14A). Since the hydrogen index also increases with increasing alginite and AOM contents (Table 1), the greater proportion of C_{27} steranes can be used to indicate greater oil proneness for this particular suite of potential source rocks. The sterane carbon number distributions should also be useful in oil-source rock correlation studies in the Sverdrup basin.

Standard thermal maturation indices were computed from the sterane data (Table 6). With an $\alpha\beta\beta/(\alpha\alpha\alpha + \alpha\beta\beta)C_{29}$ sterane ratio of 0.58, Schei Point extract 133(23) is clearly the most mature of the sample set. This conclusion is corroborated by the hopane evidence discussed above, as well as its relatively high vitrinite reflectance (0.67% R) and T_{max} (448°C) values (Table 1). For the remaining samples, the $\alpha\beta\beta/(\alpha\alpha\alpha + \alpha\beta\beta)$ ratio varies

between 0.25 and 0.46, however the coeluting C_{29} 5β(H) sterane inflates the ratio in the low maturity samples, limiting the usefulness of this parameter for these samples.

The 20S/(20R + 20S) ratio computed for the C_{29} $\alpha\alpha\alpha$ steranes appears to be a more consistent indicator of maturity for the majority of the samples, agreeing in general with maturity estimates from the hopane distributions, vitrinite reflectance and depth of burial. This parameter clearly distinguishes the very immature Ringnes formation samples 59 (33), 161 (20), 161 (21), 118 (22), 110 (24) and 139 (18) from the others (Table 6). Both the 20S/(20R + 20S) ratio and vitrinite reflectance suggest that samples 55 (8) and 45 (7) are more mature than would be expected at their relatively shallow burial depth (579 and 1204 m, respectively; Table 1). Thus there may either have been uplift or higher heat flow in this portion of the basin.

The ratio of diasteranes to regular steranes tends to increase with maturity, as seen in the ease of Schei Point sample 133 (23) (Figs. 11 and 14B, Table 6). For the remaining samples, however, this parameter varies with organic matter type, as it is consistently lower in samples enriched in alginite and AOM1 (Fig. 14B). The ratio of C_{30} hopane to C_{29} steranes is also dependent on organic matter type, at least for the Ringnes formation samples. This ratio is greater in samples with greater proportions of AOM2 (Table 1B and Table 6), which includes some bacterial lipid. This is consistent with the generally accepted idea that hopanoid compounds are also bacterially derived. This trend is less evident for the five Schei Point group samples, possibly because of the greater contribution of C_{27} steranes or because of different variety of AOM2.

3.7. Carbon isotope ratios

In order to determine if the organic matter present in the source rock samples analyzed are from the same facies, their kerogen, saturate (aliphatic) and aromatic fractions were analyzed for carbon isotope ratios ($^{13}C/^{12}C$ or δ13C). Stable carbon isotopes have been widely used as a tool for oil-oil and oil-source rock correlation (Tissot and Welte, 1984; Sofer, 1984; Sofer et al., 1986). Table 3 shows the stable carbon isotope data of the kerogen part and the saturate and the aromatic fractions of the bitumen part of the total organic matter. The saturate (aliphatics) and aromatic fractions of the extracts are plotted in Fig. 15. The dividing line drawn in Fig. 15 is from the linear equation ($\delta^{13}C_{aro} = 1.14\ \delta 13C_{sat} + 5.46$) developed by Sofer (1984) to distinguish between waxy (terrestrial) and nonwaxy (marine) oils.

The δ^{13}C values obtained from the Schei Point group fall in a relatively narrow range of - 27.71‰ to - 28.45‰ for kerogen, - 28.51‰ to - 30.35‰ for saturate fractions and - 28.10‰ to - 29.92‰ for aromatic fractions which are typical of kerogen and hydrocarbons derived from a mixture of algal/sapropelic compounds (type I/type II kerogen) and minor terrigenous plant material (type III kerogen) deposited in a marine environment (Whiticar, 1996). However, a comparison of the carbon isotope values of the samples indicates that samples (60) 17 and (98) 5 have closely similar values (i.e. they are facies-related), although sample 60 (17) has lower concentration of land plants. Terrestrial plants are typically isotopically lighter (δ^{13}C range -22‰ to -33‰) than aquatic plants (δ^{13}C = -13‰ to -27‰). The δ^{13}C values of samples from the Ringnes formation vary between -24.5 to -27.9‰ for kerogen, - 28.0 to -29.9‰ for saturates and -25.5 to -29.4‰ for aromatics. A comparison of the δ^{13}C of the saturate and aromatic fraction of the extracts of samples from the Schei Point group and Ringnes formation illustrates that a major part of the samples from the Ringnes formation are lighter compared to the samples from the Schei Point group. This data corroborates petrographic data that Ringnes samples have more influence of land plants. Whiticar (1996) suggested that carbon isotopic zonation of kerogen types is dependent on

temperature and pCO_2. The small differences in their $\delta^{13}C$ values may be due to the contribution of sapropelic or terrigenous organic matter, or to the alteration occurring during the thermal maturation.

3.8. Pyrolysis-gas chromatography/mass spectrometry

Two samples, one from the Schei Point group [sample:29 (25); TOC: 9.49%, R_o: 0.49%, HI: 733, vitrinite + inertinite: 11%] and the other from the Ringnes formation [sample:139 (18); TOC:3.06, R_o:0.45, HI:303, vitrinite + inertinite: 52%] were selected for comparison of pyrolysis-gas chromatography/mass spectrometry results (Fig. 16). The pyrolyzate of the Ringnes formation sample is characterized by a predominance of benzene and C_1 to C_3-alkylbenzenes, shown as the series of peaks labeled 'Bn' in the total ion current trace in Fig. 16 (symbols in Table 7). Toluene (peak B1) predominates. The homologous series of *n*-alk-1-enes and *n*-alkanes (labeled Δ and +) are also very important, extending to at least C_{27}. Methane, ethane and propane were not detected in the experiment due to instrumental conditions. Methylindenes (I1), naphthalene (Nn) and anthracene (Ψn) are also detected as minor components. Phenol and C_1 to C_3-alkylphenols, labeled ΦO, are prominent constituents. Thiophenes (e.g., Θ1) make only a minor contribution.

The Schei Point group sample yielded roughly three times more pyrolyzate per unit weight than the Ringnes group sample. Although the total ion current trace of the Schei Point sample (Fig. 16) closely resembles that of the other sample in its distribution of the aromatic and aliphatic hydrocarbons, the major point of distinction shows that it has a significantly lower abundance of phenols. This particular Ringnes example is relatively more oil-prone and enriched in alginite and AOM1 than other samples from the same formation (Table lB). The other Ringnes samples would likely produce distinctive pyrolyzates - enriched in phenols and depleted in aliphatics.

The quantitation results (Table 8) confirm the predominantly aliphatic character of the Arctic samples, with aliphatic/benzene ratios that are nearly the same: 3.35 for the Ringnes and 3.25 for the Schei Point. However, the Ringnes sample is significantly more phenolic, as shown by the phenol/benzene ratio of 0.49 (three times that of the Schei Point sample). Phenols are typical of pyrolysis products of vitrinite (Kruge and Bensley, 1994), indicating a greater terrestrial influence on the Ringnes kerogen, as confirmed by petrographic examination (Table 1B).

In conclusion, the Schei Point sample is more oil-prone than the Ringnes sample which corroborates petrographic data.

4. Summary and conclusions

Analyzed samples from both the Schei Point group and the Ringnes formation are organic-rich (> 2% TOC). Most samples from the Schei Point contain more than 75% amorphous organic matter (AOM1 and AOM2) and alginite (*Tasmanales, Nostocopsis, Leiosphaeridia*, acritarch and dinoflagellate) with a varying proportion of vitrinite and inertinite (terrestrial input) . Organic facies characteristics suggest that most of these sediments were deposited in a marine anoxic to dysoxic environment with an abundance of phytoplankton; this setting received a periodic influx of terrestrial organic matter. Most samples lie within immature to early mature zones (0.4 to 0.7% R_o) . Many samples are kerogen type I- IIA and IIA (II of Tissot and Welte, 1984); sample 60 (17) is of kerogen type I. All analyzed samples are considered as major liquid hydrocarbon source rock. The Ringnes samples have mixed terrestrial (vitrinite, inertinite and exinite) and marine [alginite (*Tasmanales, Botryococcus*, etc.), AOM1 and AOM2] which are partially oxidized. The

samples show a maturity of 0.44% to 1.40% R_o. Most of these samples have a vitrinite reflectance of 0.45% to 0.75% R_o. They represent multiple source rocks of kerogen types IIA-IIB (II-III of Tissot and Welte, 1984), IIB (II-III) and III, the majority of which can generate condensate and gas (kerogen type IIB and III).

The bitumen content varies between 9 to 46 mg HC/g TOC and 10 to 63 mg HC/g TOC for the Ringnes and Schei Point samples, respectively. In general, the Schei Point samples have higher hydrocarbon content, saturate/aromatic ratios, lower CPI, pristane/phytane and pristane/*n*-C_{17} compared to the Ringnes samples. This data suggests that such variations are controlled mainly by organic facies than maturity since the samples compared were of similar maturity.

Sterane carbon number distributions in the Ringnes samples show no major variations and are consistent with a mixed algal and terrestrial organic matter type. There are some variations in hopane carbon number distributions, but these are apparently a function of thermal maturity, rather than genetic differences among samples. In contrast, there is considerable variation in the distributions of sterane and hopane isomers, mostly attributable to maturation effects. Immature samples are clearly distinguished from the mature samples by standard sterane and hopane isomer ratios. Triterpane and sterane distribution patterns and related parameters (C_{27}-C_{35} homologs of 17α,21β hopanes and tricyclic terpanes of Schei Point samples) suggest that samples (44) 11 and (60) 17 are less mature than samples (29) 25, 133 (23) and (97) 5. Sterane carbon number distributions are consistent with a mixture of algal (sapropelic) and humic (terrestrially derived) kerogens, with sapropelic kerogen being the dominant part. This finding, confirmed by the strong presence of C_{30}-sterane, suggests a marine depositional environment. The Schei Point group and the Ringnes formation organic extracts can be readily distinguished by their biomarker distributions, regardless of maturity level. The most striking differences are the greater relative abundances of tricyclic terpanes, C_{33}-C_{35} extended hopanes and C_{27} regular steranes in the Schei Point group samples. These features should be exploited in oil-source rock correlation studies in this basin.

Carbon isotope ratios confirm the gas chromatography and GC-MS results, showing $\delta^{13}C$ values typical of hydrocarbons generated from a mixture of marine-(type I/II) and terrestrially-derived (type III) organic matter deposited in a near-shore marine environment under weak dystrophic conditions. The Schei Point samples show a greater marine influence compared to those of the Ringnes formation samples. The small difference in $\delta^{13}C$ values may be due to the contribution of sapropelic and/or terrigenous land plants, or possibly due to alteration occurring during thermal maturation.

Pyrolysis-gas chromatography/mass spectrometry of two samples of similar maturity, one each from the Schei Point group and Ringnes formation, showed that the Schei Point samples generated three times more pyrolyzate than did the Ringnes sample. Both samples have a dominant aliphatic character, although the Ringnes sample is more phenolic than the Schei Point sample, indicating a greater terrestrial influence.

Acknowledgements

The manuscript was greatly improved by critical reviews from Coleman R. Robison and an anonymous reviewer. The authors acknowledge the help of the drafting section of the Nova Scotia Department of Natural Resources, Halifax, Nova Scotia, Canada.

References

Baker, D.A., Illich, H.A., Martin, S.J., Landin, R.R., 1975. Hydrocarbon source potential of sediments in the Sverdrup basin. Mem. Can. Soc. Petrol. Geol. 4, 545- 556.

Balkwill, H.R., 1978. Evolution of Sverdrup basin, arctic Canada. Bull. Am. Assoc. Petrol. Geol. 62, 1004-1028.

Brooks, P.W., Embry, A.F., Goodarzi, F., Stewart, R., 1992. Organic geochemistry and biological marker geochemistry of Schei Point group (Triassic) and recovered oils from the Sverdrup basin (arctic islands, Canada). Bull. Can. J. Petrol. Geol. 40 (3), 173- 187.

Connan, J., Cassou, A.M., 19 80. Properties of gases and petroleum liquids derived from terrestrial kerogen at various maturation levels. Geochim. Cosmochim. Acta 44, 1- 23.

Embry, A.F., 1984. The Schei Point and Blaa Mountain groups (middle to upper Triassic), Sverdrup basin, Canadian arctic archipelago. In: Geol. Surv. Canada Current Res., Part B, Paper 84-lB, pp. 327- 336.

Embry, A.F., 1989. Correlation of Upper Paleozoic and Mesozoic sequences between Svalbard, Canadian arctic archipelago and northern Alaska. In: Collinson, J.D. (Ed.), Correlation Petroleum Exploration, Norwegian Petroleum Society. Graham and Trotman, London, pp. 89-98.

Embry, A.F., 1991, Mesozoic history of the arctic islands. In: Trettin, H.P. (Ed.) Innuitian orogeny and arctic platform of Canada and Greenland. Geological Survey of Canada volume, Geology of Canada 3, ch. 14, pp. 369- 434.

Espitalie, J., Deroo, Cr., Marquis, F., 1985. Rock-Eva] pyrolysis and its applications. Report Institut Français du Petrole No. 33878, 72 pp.

Fowler, M.R., Brooks, P.W., 1990. Organic geochemistry as an aid in the interpretation of the history of oil migration into different reservoir at the Hibernia K-18 and Ben Nevis I-45 wells, Jeanne d' Arc basin, offshore eastern Canada. Org. Geochem. 16, 461- 475.

Gentzis, T., Goodarzi, F., 1992a. The source rock potential and thermal maturity of the sedimentary succession in the Drake and Hecla hydrocarbon fields, Mesville island, Canadian arctic archipelago. In: Vorren, T.O., et al. (Eds.), Arctic Geology and Petroleum Potential, NPF Special Publication 2. Elsevier Science, Amsterdam, pp. 159-171.

Gentzis, T., Goodarzi, F., 1992b. Thermal maturity and source rock potential of the sedimentary succession from the Drake field, Sverdrup basin, arctic Canada . J. Petrol. Geol. 16 (1), 33- 54.

Gentzis, T., Goodarzi, F., 1993a. Thermal maturity and source rock potential in northwestern Melville island, arctic Canada. Energy Sources 14, 423- 442.

Gentzis , T., Goodarzi, F., 1993b. Maturity studies and source rock potential in the southern Sverdrup basin, arctic Canada. Int. J. Coal Geol. 24, 141- 177.

Gentzis, T., de Freitas, T., Goodarzi, F., Melchin , M., Lenz, A., 1996. Thermal maturity of lower Paleozoic sedimentary successions in arctic Canada. Bull. Am. Assoc. Pet. Geol. 80 (7), 1065-1084.

Goodarzi, F., Stasiuk, L.D., 1987. Amorphous kerogen: bituminite in the second white speckled shales southem Saskatchewan. Geol. Surv. Can. Current Res, Part A, Paper 87-l A, pp. 349-352.

Goodarzi, F., Davies, G., Nassichuk , W.W., Snowdon, L.R., 1987. Organic petrology and Rock-Eva! pyrolysis of lower carboniferous Emma fiord formation in Sverdrup basin, Canadian arctic archipelago . Mar. Petrol. Geol. 4, 132-145.

Goodarzi, F., Brooks, P.W., Embry, A.F., 1989. Regional maturity as determined by organic petrography and geochemistry of the Schei Point group (Triassic). Mar. Petrol. Geol. 6 (4), 290- 303.

Goodarzi, F., Gentzis, T., Embry, A.F., Osadetz, K.G., Skibo, D.N., Stewart, K.R., 1992. Evaluation of maturity and source rock potential in the Loughheed island area of the central Sverdrup basin, arctic Canada. In: Vorren, T.O., et al. (Eds.), Arctic Geology and Petroleum Potential, NPF Special Publication 2. Elsevier Science, Amsterdam, pp. 147-157.

Henao-Londono, D., 1977. A preliminary geochemical evaluation of the arctic islands. Bull. Can. Petrol. Geol. 25, 1059-1084.

Horstad, I., Larter, S.R., Dypvik, H., Aagaard, P., Bjomvik, A.M., Johansen, P.E., Eriksen, S., 1990. Degradation and maturity controls on oil field petroleum column heterogeneity in the Gullfaks field, Norwegian North Sea. Org. Geochem. 16, 497- 510.

Huang , W.-Y., Meinschein, W.G., 1979. Sterols as ecological indicators. Geochim. Cosmochim. Acta 43, 739- 745.

Jones, R.W., 1987. Application of organic facies for hydrocarbon potential. In: Brooks, J. (Ed.), Advances in Petroleum Geochemistry 2. Academic Press, pp. 1- 90.

Kruge, M.A., Bensley, D.F., 1994. Flash pyrolysis-gas chromatography-mass spectrometry of lower Kittanning vitrinites: changes in distributions of polyaromatic hydrocarbons as a function of coal rank. In: Mukhopadhyay, P. K., Dow, W.G. (Eds.), Vitrinite reflectance as a maturity Parameters - Applications and Limitations. American Chemical Society Symposium Serie 570, Washington, D.C., pp. 136- 148.

Leith, T.L., Weiss , H.M., Mork, A., Arhus, N., Elvebakk, G., Embry, A.F., Brooks, P.W., Stewart, K.R., Pchelina, T.M., Bro, E.G., Verba, M.L., Danyushevskaya, A., Borisov, A.V., 1992. Mesozoic hydrocarbon source rocks of the Arctic region. In: Vorren, T.O., et al. (Eds.), Arctic Geology and Petroleum Potential, NPF Special Publication 2. Elsevier Science, Amsterdam, pp. 1-25.

Moldowan, J.M., Fago, F.J., Carlson, R.M.K., Young, D.C., Van Duyne, G., Clardy, J., Schoeel, M., Pillinger, C.I., Watt, D.S., 1991. Rearranged hopanes in sediments and petroleum. Geochim. Cosmochim. Acta 55, 3333- 3353. .

Monier, F., Powell, T.G., Snowdon, L.R., 1981. Qualitative and quantitative aspects of gas generation during maturation of sedimentary organic matter: Examples from Canadian frontier basins. In: Bjoroy, M., et al. (Eds.), Advances in Organic Geochemistry 1981. Wiley, Chichester, pp. 487-495.

Mukhopadhyay, P.K ., 1989. Characterization of amorphous and other organic matter types by microscopy and pyrolysis-gas chromatography. Org. Geochem. 14 (3), 269- 284.

Mukhopadhyay, P. K., 1992a. Organic facies and source rock characterization of rocks from the arctic. SSC Report. File No. XSG91-00073-(607).

Mukhopadhyay, P.K., 1992b. Maturation of organic matter as revealed by microscopic methods: applications and limitations of vitrinite reflectance and continuous spectral and pulsed laser fluorescence spectroscopy. In: Chilingarian, G.V., Wolf, K. (Eds.), Diagenesis III: Developments in Sedimentology 47. Elsevier Publication, Amsterdam, pp. 435 - 510.

Mukhopadhyay, P.K., 1993. Organic geochemistry including maturation study of source rocks from Arctic Canada. SSC Report. File No. XSG92-00029-(604).

Mukhopadhyay, P.K., Wade, J.A., 1990. Organic facies and maturation of sediments from the three Scotian shelf wells. Bull. Can. Petrol. Geol. 38 (4), 407- 424.

Mukhopadhyay, P.K., Hagemann, H.W., Gormly, J.R., 1985. Characterization of kerogens as seen under the aspect of maturation and hydrocarbon generation. Erdoel Kohle Erdgas Petrochem. 38 (1), 7-18.

Mukhopadhyay, P.K., Wade, J.A., Kruge, M.A., 1995. Organic facies and maturation of Cretaceous/Jurassic rocks and possible oil-source rock correlation based on pyrolysis of asphaltenes, Scotian basin, Canada. Org. Geochem. 22 (1), 85-104.

Powell, T.G., 1978. An assessment of the hydrocarbon source potential of the Canadian Arctic. Geological Survey of Canada Paper 78-12, 82 pp.
Seifert, W.K., Moldowan, J.M., 1980. The effect of thermal stress on source-rock quality as measured by hopane stereochemistry. In: Douglas, A.G., Maxwell, J.R. (Eds.), Advances in Organic Geochemistry 1979. Pergamon Press, Oxford, pp. 229-237.
Senftle , J.T., Brown, J.H., Larter, S.R., 1987. Refinement of organic petrographic methods for kerogen characterization. Int. J. Coal. Geol. 7, 105-118.
Senftle, J.T., Landis, C.R., McLaughlin, R., 1993. In: Engels, M.H., Macko, S. (Eds.), Organic Geochemistry. Plenum Press, New York, pp. 377-396.
Snowdon, L.R., Roy, K.J., 1975. Regional organic metamorphism in Mesozoic strata of the Sverdrup hasin. Bull. Can. Pet. Geol. 23, 131-148.
Sofer, Z., 1984. Stable carbon isotope compositions of crude oils: Application to source depositional environments and petroleum alteration. Bull. Am. Assoc. Petrol. Geol. 68 (1), 31-49.
Sofer, Z., Zumberge, J.E., Lay, V., 1986. Stable carbon isotopes and biomarkers as tools in understanding genetic relationship, maturation, biodegradation and migration of crude oils in the northern Peruvian oriente (Maranon) basin. Org. Geochem. 10, 377-389.
Stach, E., Mackowsky, M.Th., Teichmuller, M., Taylor, G.H., Chandra, D., Teichmuller , R., 1982. Texthook of Coal Petrology. 3rd Ed. Borntraeger, Stuttgart, 536 pp.
Stasiuk , L.D., 1991. Organic Petrology and Petroleum Formation in Paleozoic Rocks of Northern Williston Basin, Canada. Ph.D. dissertation, University of Regina, 313 pp.
Stasiuk, L.D., Osadetz, K.G., Goodarzi, F., Gentzis, T., 1991. Organic rnicrofacies and basinal tectonic control on source rock accumulation: a microscopic approach with examples from an intracratonic and extensional basin. Int. J. Coal Geol. 19, 457-481.
Stewart, K.R., Embry, A.F., Goodarzi, F., Ski ho, D.N., 1992. Evaluation of organic maturity and hydrocarbon source potential of the Ringnes formation, Sverdrup basin, arctic Canada. Org. Geochem. 18 (3), 317-332.
Teichmuller, M., 1986. Organic petrology of source rocks, history and state of the art. Org. Geochem. 10 (1-3), 581-599.
Teichmuller, M., Ottenjann, K., 1977. Liptiniten und Lipoids Stoffe in einem Erdolmuttergestein. Erdoel Kohle 3, 387-398.
Tissot B.P., Weite D.H., 1984. Petroleum Formation and Occurrence. Springer Verlag, Berlin, 699 pp.
Van Gijzel, P., 1981. Characterization and identification of kerogen and bitumen and determination of thermal maturation by means of qualitative and quantitative microscopical techniques. In: Society of Economic Paleontologists and Mineralogists Short Course Note 7, pp. 159- 207.
Whelan, J.K., Thompson-Rizer, C.L., 1993. In: Engel, M.H., Macko, S.A. (Eds.), Organic Geochemistry. Plenum Press, New York, pp. 289- 352.
Whiticar, M.J., 1996. Stable isotope geochemistry of coals, humic kerogens and related natural gases. Int. J. Coal. Geol. 32 (1- 4), 191-216.

Table 1. Sample and well numbers, depth, formation or member and data on total organic carbon (TOC in wt%), vitrinite reflectance (% R_o), S1, S2 and hydrogen index from Rock-Eval pyrolysis (partial data), maceral composition and kerogen type of rocks from the Schei Point group and the Ringnes formation.

Sample location[a] (number)	Borehole number	Depth (m) and formation	TOC (wt%)	Vit. refl. (% R_o)	S_1 (RE)	S_2 (RE)	HI (RE)	Maceral composition (vol%)							Kerogen type
								Vit (%)	Int (%)	Exin (%)	Alg (%)	AOM1 (%)	AOM2 (%)	Bit (%)	
(A) Schei Point group															
16 (32)	Elf Wilkens E-60	1005.8 (Eden Bay)	2.66	0.51	0.9	16.26	611	13	14		5	54	14		II (IIA)
20 (18)	Elf Jameson Bay C-31	1130.9 (Eden Bay)	5.07	0.48	1.05	32.10	633	15	4	1	17	18	45		II (IIA)
29 (25)	BP Panarctic Satellite F-68	862.6 (Cape Richards)	9.49	0.49	2.07	73.40	773	7	4		13	43	33		I–II (IIA)
29 (26)	BP Panarctic Satellite F-68	877.8 (Eden Bay)	9.52	0.54	2.57	65.03	683	3	2		7	35	52	1	I–II (IIA)
44 (11)	Tenneco Drake Point F-16	1295.4 (Eden Bay)	4.97	0.53	1.00	31.93	642	2	2		5	9	81	1	II (IIA)
52 (12)	BP Panarctic Emerald K-33	1591.1 (Eden Bay)	7.74	0.50	0.19	55.50	722	1	1		9	17	70	2	I–II (IIA)
58 (22)	Panarctic Tenneco Pollux G-60	1371.6 (Murray harbour)	4.06	0.54	1.20	19.76	494	12	7	10	10	1	59	1	II (IIA)
60 (17)	Elf Intepid Inlet H-49	804.7 (Cape Richards)	7.93	0.48	1.26	74.38	937	3	1		14	67	14	1	I
64 (29)	Dome Arctic Ventures SutherlandO-23	1661.2 (Hoyle Bay)	4.05	0.50	1.59	22.69	560	6	6	5	6	1	75	1	II (IIA)
72 (10)	Panarctic et al. Drake Point D-68	1338.1 (Eden Bay)	4.57	0.56	1.32	30.03	657	3	2	4	6	14	70	1	II (IIA)
73 (1)	Elfex Andreasen L-32	1051.6 (Cape Richards)	9.80	0.55	2.27	71.43	728	6	3		7	72	10	2	I–II (IIA)
97 (5)	Panarctic et al. Chads Creek B-64	1478.3 (Cape Richards)	5.74	0.46	1.27	40.64	708	7	3		7	75	7	1	I–II (IIA)
98 (7)	Panarctic et al. Collingwood K-33	1850.1 (Eden Bay)	5.40	0.52	1.42	34.93	647	9	3		5	25	57	1	II (IIA)
100 (21)	Panarctic Temneco et al. Pat Bay A-72	2828.5 (Eden Bay)	3.00	0.46	1.00	16.54	551	16	4	5	8	4	60	1	II (IIA)

Table 1 (cont'd)

133 (23)	Panarctic et al. AIEG Roche Point J-43	2682.2 (Eden Bay)	3.80	0.67	1.66	12.6	332	15	7	13	3	1	60	1	matured	II–III (IIA)
166 (30)	Panarctic et al. Grenadier A-26	1905.0 (Murry harbour)	5.06	0.52	1.05	26.82	530	5	2	8	3	1	80	1	matured	II (IIA)
83 (20)[b]	Gulf WC et al. Neil O-15	1051.6 (Murray harbour)	2.46	0.90	1.14	7.39	300	14	6	10	2	1	64	3	II–III	
94 (27)[b]	Panarctic Dome Sherard Bay F-14	1277.1 (Eden Bay)	3.88	0.51	1.11	18.62	480	6	6	12	7	2	66	1	II (IIA)	
163 (19)[b]	Panarctic et al. Marryatt K-71	1638.0 (Eden Bay)	3.00	0.54	1.21	16.53	551	19	4	17	14	2	40			
(B) Ringnes formation																
31 (2)	Panarctic Tenneco et al. Kristoffer Bay B-06	920.5	3.25	0.56	0.78	7.57	232	34	10	20	8		25	2	II–III (IIB)	
35 (12)	Panarctic Gulf Dumbbells E-49	2118.4	3.06	0.58	0.94	10.14	331	26	14	15	8	4	32	1	II–III (IIB)	
35 (13)	Panarctic Gulf Dumbbells E-49	2377.4	3.72	0.71	1.16	8.72	234	40	15	18	2		24	1	II–III (IIB)	
41 (32)	Panarctic Gulf W. Amund I-44	435.5	3.43	0.59	0.35	3.86	112	60	15	18	6		1		III	
45 (6)	Panarctic Dome Tenneco Dome Bay P-36	1082.0	2.75	0.57	0.67	7.79	280	32	12	8	16	2	29	1	II–III (IIB)	
45 (7)	Panarctic Dome Tenneco Dome Bay P-36	1204.0	4.96	0.70	1.38	11.42	230	45	12	17	3		22	1	II–III (IIB)	
55 (8)	Panarctic Dome Louise O-25	579.1	3.20	0.60	1.23	10.72	335	22	16	4	2	8	47	1	II–III (IIA)	
59 (33)	dome Arctic Ventures Wallis K-62	1615.4	6.44	0.52	0.49	10.33	160	56	24	3	1	1	15		III (IIB)	
86 (26)	Sun GA KRC Panarctic Elve M-40	883.9	2.69	0.53	0.29	4.84	179	35	20	17	10		16	2	II–III (IIB)	
86 (27)	Sun GA KRC Panarctic Elve M-40	1066.8	5.33	0.53	0.64	8.57	160	50	17	8	8		17		II–III (IIB)	
110 (24)	Panarctic Mocklin Point D-23	960.1	4.31	0.46	0.47	13.99	324	28	6	9	29	7	20	1	II–III (IIB)	
118 (22)	Panarctic Tenn. Sun Dome Jackson	914.4	6.16	0.50	0.69	10.61	172	46	9	6	3		35	1	II–III (IIB)	
139 (18)	Panarctic et al. Noice D-41	1015.0	3.06	0.45	0.43	9.30	303	38	14	4	11	8	24	1	II–III (IIB)	
161 (20)	Panarctic et al. Sculpin K-08	939.0	4.20	0.47	0.35	10.73	255	33	12	17	9	10	18	1	II–III (IIB)	
161 (21)	Panarctic et al. Sculpin K-08	1035.0	7.43	0.58	0.65	13.33	179	45	13	14	1		26	1	II–III (IIB)	
69 (31)[b]	Imp. Panarctic Union PPL E. Amund M-05	435.9	2.30	1.40	0.17	0.05	2	52	35	2	3		4	4	matured	
157 (5)[b]	Panarctic Dome et al. Hoodoo N-52	1101.0	2.98	0.88	0.48	1.22	40	55	29	2	1		12	1	II–III (IIB) III	

TOC = total organic carbon; Vit. refl. = mean random vitrinite reflectance; RE= Rock-Eval pyrolysis; S1 = hydrocarbons released from source rocks and measured in mg/g of rock at 300°C from Rock-Eval pyrolysis; S2 = hydrocarbons generated from source rocks and measured in mg/g of rock at temperatures between 300-550°C from Rock-Eval pyrolysis; HI= hydrogen index in mg HC/g TOC derived from Rock-Eval pyrolysis; vit = vitrinite; int = inertinite; exin = exinite; alg = alginite; AOM 1 = amorphous organic matter (liptinite) number 1 derived from the biodegradation of larger algae; AOM2 = amorphous organic matter (liptinite) number 2 derived from biodegradation of other phytoplanktons (acritarch, dinoflagellates, etc.) and/or exinite (spore, pollen, cutinite, suberinite); bit = solid bitumen.

[a] Well locations are shown in Fig. 1.

[b] Samples used only for organic petrography, TOC and Rock-Eval pyrolysis.

Table 2. Bitumen extraction and liquid chromatography (% saturates, aromatics and polar components and saturate/aromatics and saturate/polar ratios) data of samples from the Schei Point group and Ringnes formation.

Sample No.	Borehole No.	Depth (m)	TOC (wt%)	R_o	Bitumen content (mg/g TOC)	Gross composition (%)			Sat/ arom	Sat/ polar
						saturates	aromatics	NSO'S		
Schei Point group										
16 (32)	Wilkins A-60	1005.8	2.66	0.51	30.1	67.8	10.7	21.6	6.3	3.1
20 (18)	Jameson Bay C-31	1130.9	5.07	0.48	9.9	50.0	5.8	44.2	8.6	1.1
29 (25)	satellite F-68	877.8	9.49	0.49	28.5	56.7	22.0	21.3	2.6	2.7
44 (11)	Drake Point F-16	1295.4	4.97	0.53	16.1	23.6	16.8	59.6	1.4	0.4
52 (12)	Emerald K-33	1591.1	7.74	0.50	63.3	43.8	28.8	27.4	1.5	1.6
58 (22)	Pollux G-60	1371.6	4.06	0.54	17.1	57.6	12.4	30.0	4.6	1.9
60 (17)	Intrepid inlet H-49	804.7	7.93	0.48	20.2	30.1	23.1	46.8	1.3	0.6
64 (29)	Sutherland 0-23	1661.2	4.05	0.50	34.6	57.0	26.0	17.0	2.2	3.4
72 (10)	Drake Point D-68	1338.1	4.57	0.56	19.7	53.8	8.1	38.0	6.6	1.4
73 (1)	Andreasen L-32	1051.6	9.80	0.55	14.3	58.1	20.5	21.4	2.8	2.7
97 (5)	Chads Creek B-64	1478.3	5.74	0.46	13.9	40.3	13.4	46.3	3.0	0.9
98 (7)	Collingwood K-33	1850.1	5.40	0.52	27.8	36.8	34.9	28.3	1.1	1.3
100 (21)	Pat Bay A-72	2828.5	3.00	0.46	56.5	48.9	33.8	17.3	1.4	2.8
133 (23)	Roche Point I-43	2682.2	3.80	0.67	34.2	52.9	16.9	30.2	3.1	1.8
166 (14)	Granadier A-26	1905.0	5.06	0.52	25.7	34.3	19.9	45.8	1.7	0.7
Ringnes formation										
31 (2)	Kristoffer Bay B-06	920.5	3.25	0.56	23.0	30.0	19.0	51.0	1.6	0.6
35 (12)	Dumbbells E-49	2118.4	3.06	0.51	41.0	47.0	17.0	36.0	2.8	1.3
35 (13)	Dumbbells E-49	2377.4	3.72	0.71	22.0	32.0	26.0	42.0	1.3	0.8
41 (32)	W. Amund 1-44	435.9	3.43	0.59	9.0	35.0	17.0	48.0	2.0	0.7
45 (6)	Dome Bay P-36	1082.0	2.75	0.57	29.0	36.0	18.0	47.0	2.0	0.8
45 (7)	Dome Bay P-36	1204.0	4.96	0.70	11.0	48.0	14.0	38.0	3.5	1.2
55 (8)	Louise O-25	579.1	3.20	0.60	46.0	52.0	17.0	31.0	3.0	1.7
59 (33)	Wallis K-62	1615.4	6.44	0.52	16.0	24.0	28.0	48.0	0.8	0.5
86 (26)	Elve M-40	883.9	2.69	0.53	21.0	5.0	17.0	77.0	0.3	0.1
86 (27)	Elve M-40	1066.8	5.33	0.53	22.0	24.0	33.0	44.0	0.7	0.6
110 (24)	Mocklin Point D-23	960.1	4.31	0.46	18.0	29.0	24.0	47.0	1.2	0.6
118 (22)	Jackson G-16A	914.4	6.16	0.50	20.0	18.0	25.0	58.0	0.7	0.3
139 (18)	Noice D-41	1015.0	3.06	0.45	16.0	35.0	15.0	50.0	2.3	0.7
161 (20)	Sculpin K-08	939.0	4.20	0.58	15.0	27.0	26.0	48.0	1.0	0.6
161 (21)	Sculpin K-08	1035.0	7.43	0.47	15.0	26.0	27.0	47.0	0.9	0.5

Table 3. CPI (carbon preference index) and isoprenoid/*n*-alkane ratios and stable carbon isotope data of bitumen (saturate and aromatic fractions) and kerogen of various samples from the Schei Point group and Ringnes formation.

Sample No.	Borehole No.	Depth (m)	CPI	Pristane /phytane	Pristane/ nC_{17}	Phytane/ nC_{18}	$\delta^{13}C_{PDB}$‰ kerogen	$\delta^{13}C_{PDB}$‰ saturate	$\delta^{13}C_{PDB}$‰ aromatics
Schei Point group									
29 (25)	Satellite F-68	877.8	1.05	1.19	1.10	0.97	−28.45	−30.35	−29.92
44 (11)	Drake Point F-16	1295.4	1.09	0.78	1.20	2.40	−28.26	−28.99	−28.51
60 (17)	Intrepid Inlet H-49	804.7	1.21	0.68	1.70	2.02	−27.79	−28.51	−28.79
98 (7)	Collingwood K-33	1850.1	1.15	1.16	1.33	1.29	−27.71	−28.51	−28.10
133 (23)	Roche Point J-43	2682.2	1.00	1.10	0.90	0.86	−28.41	−29.70	−29.04
Ringnes formation									
35 (12)	Dumbbells F-49	2118.4	1.30	2.28	1.73	0.87	−27.3	−29.5	−28.2
35 (13)	Dumbbells F-49	2377.4	1.17	2.57	1.03	0.39	−25.6	−27.6	−25.6
45 (7)	Dome Bay P-36	1204.0	1.24	2.62	1.24	0.53	−25.9	−28.2	−26.9
55 (8)	Louise O-25	579.1	1.17	1.88	1.21	0.68	−27.9	−29.9	−28.8
59 (33)	Wallis K-62	1615.4	1.64	2.09	1.10	0.66	−24.5	−27.9	−25.5
110 (24)	Mocklin Point D-23	960.1	1.72	1.96	3.54	2.54	−27.7	−29.7	−29.3
118 (22)	Jackson G-16A	914.4	1.81	2.93	1.89	0.88	−24.6	−28.0	−25.5
139 (18)	Noice D-41	1015.0	1.59	2.18	2.92	1.63	−27.3	−29.6	−29.2
161 (20)	Sculpin K-08	939.0	2.14	1.24	3.74	3.39	−27.5	−29.9	−29.4
161 (21)	Sculpin K-08	1035.0	1.92	2.73	1.68	1.09	−25.2	−28.4	−26.3

Table 4. Key for tricyclic, tetracyclic and pentacyclic terpanes identification (m/z 191 fragmentograms).

Code	Compound	Carbon #
0	C_{20}-tricyclic terpane	20
1	C_{21}-tricyclic terpane	21
2	C_{22}-tricyclic terpane	22
3	C_{23}-tricyclic terpane	23
4	C_{24}-tricyclic terpane	24
5	C_{25}-tricyclic terpane	25
Z4	C_{24}-tetracyclic terpane	24
6a	C_{26}-tricyclic terpane	26
6b	C_{26}-tricyclic terpane	26
A	C_{28}-tricyclic terpane #1	28
B	C_{28}-tricyclic terpane #2	28
C	C_{29}-tricyclic terpane #1	29
D	C_{29}-tricyclic terpane #2	29
E	18α-22,29,30-trisnorneohopane (Ts)	27
F	17α-22,29,30-trisnorhopane (Tm)	27
G	17β-22,29-30-trisnorhopane	27
10a	C_{30}-tricyclic terpane #1	30
10b	C_{30}-tricyclic terpane #2	30
11a	C_{31}-tricyclic terpane #1	31
11b	C_{31}-tricyclic terpane #2	31
K	17α,21 13-30-norhopane	29
$C_{29}T_s$	18α-30-norneohopane	29
C30	17α-diahopane	30
L	17β-21α-30-normoretane	29
N	17α,21β-hopane	30
O	17β,21α-moretane	30
P	22*S*-17α,21β-30-homohopane	31
Q	22*R*-17α,21β-30-homohopane	31
14a	C_{34}-tricyclic terpane #1	34
S	17β,21α-homomoretane	31
14b	C_{34}-tricyclic terpane #2	34
T	22*S*-17α,21β-30-bishomohopane	32
U	22*R*-17α,21β-30-bishomohopane	32
15a	C_{35}-tricyclic terpane #1	35
15b	C_{35}-tricyclic terpane #2	35
V	17β,21α-C_{32}-bishomomoretane	32
WS	22*S*-17α,21β-30,31,32-trishomohopane	33
WR	22*R*-17α,21β-30,31,32-trishomohopane	33
XS	22*S*-17α,21β-30,31,32,33-tetrahomohopane	34
XR	22*R*-17α,21β-30,31,32,33-tetrahomohopane	34
YS	22*S*-17α,21β-30,31,32,33,34-pentahomohopane	35
YR	22*R*-17α,21β-30,31,32,33,34-pentahomohopane	35

Table 5. Key for steranes identification (m/ z 217 mass chromatogram).

Code	Compound	Carbon #
1	13β,17α-diacholestane (20S)	27
2	13β,17α-diacholestane (20R)	27
3	13α,17β-diacholestane (20S)	27
4	13α,17β-diacholestane (20R)	27
5	24-methyl-13β,17α-diacholestane (20S)	28
6	24-methyl-13β,17α-diacholestane (20R)	28
7D	24-methyl-13α,17β-diacholestane (20S)	28
7	14α,17α-cholestane(20S)	27
8 + 8D	14β,17β-cholestane(20R) + 24-ethyl-13β,17α-diacholestane (20S)	27 + 29
9	14β,17β-cholestane (20S)	27
9D	24-methyl-13α,17β-diacholestane (20R)	28
10	14α,17α-cholestane (20R)	27
11	24-ethyl-13β,17α-diacholestane (20R)	29
12	24-ethyl-13α,17β-diacholestane (20S)	29
13	24-methyl-14α,17α-cholestane (20S)	28
14 + 14D	24-methyl-14β,17β-cholestane(20R) + 24-ethyl-13α,17β-diacholestane (20R)	28 + 29
15	24-methyl-14β,17β-cholestane (20S)	28
16	24-methyl-14α,17α-cholestane (20R)	28
17	24-ethyl-14α-cholestane (20S)	29
18	24-ethyl-14β,17β-cholestane (20R)	29
19	24-ethyl-14β,17β-cholestane (20S)	29
20	24-ethyl-14α,17α-cholestane (20R)	29
21A	24-*n*-propylcholestanes	30

Table 6. Biomarker ratios for Schei Point group and Ringnes formation rock extracts. Quantitations performed on m/z 191 and 217 mass fragmentograms. Ratios of various sterane and triterpanes.

Sample	20S/(20R + 20S)	$\alpha\beta\beta/(\alpha\alpha\alpha + \alpha\beta\beta)$	Diasteranes/	C_{30} $\alpha\beta$ hopanes/	($\alpha\alpha\alpha$ 20R steranes)		
	C_{29} $\alpha\alpha\alpha$ steranes	C_{29} steranes	reg. steranes	C_{29} reg. steranes	%C_{27}	%C_{28}	%C_{29}
Schei Point group							
(44) 11	0.11	0.25	0.20	0.6	33.4	24.3	42.3
(29) 25	0.28	0.28	0.28	0.8	32.7	24.2	43.1
(133) 23	0.33	0.58	0.65	1.3	34.7	25.0	40.3
(60) 17	0.09	0.27	0.12	0.5	36.8	27.8	35.4
(98) 7	0.27	0.32	0.29	0.9	32.4	23.5	44.1
Ringnes formation							
(45) 7	0.46	0.38	0.51	4.3	28.8	18.0	53.2
(55) 8	0.49	0.46	0.40	2.9	25.5	17.1	57.4
(35) 12	0.46	0.39	0.46	1.2	26.2	19.8	54.1
(35) 13	0.47	0.44	0.47	3.7	22.2	19.3	58.5
(139) 18	0.28	0.28	0.44	0.8	31.8	20.7	47.5
(161) 20	0.21	0.36	0.49	0.7	30.6	20.7	48.7
(161) 21	0.21	0.39	0.41	1.9	26.1	18.9	55.1
(118) 22	0.22	0.36	0.48	2.1	16.6	18.4	65.0
(110) 24	0.27	0.30	0.47	0.6	31.5	21.1	47.4
(59) 33	0.18	0.42	0.42	1.8	20.8	19.4	59.9

Table 7. Py-GC/MS peak identifications for Figure 16 and ions used in quantitation. 'NQ ' indicates that these compounds were not quantitated for this study.

Symbol	Compound	Ion (m/z)
Δ	*n*-alk-1-enes	55
+	*n*-alkanes	57
B0	benzene	78
B1	toluene	92
B2	C_2-alkylbenzenes	106
B3	C_3-alkylbenzenes	120
B4	C_4-alkylbenzenes	134
N0	naphthalene	128
N1	C_1-alkylnaphthalenes	142
N2	C_2-alkylnaphthalenes	156
Φ0	phenol	128
Φ1	C_1-alkylphenols	142
Φ2	C_2-alkylphenols	156
I0	indene	NQ
I1	methylindenes	NQ
Θ1	2-methylthiophene	NQ
Y0	phenanthrene, anthracene	NQ

Table 8. Py-GC/MS compound class ratios, based on the summed quantitation results for aliphatic hydrocarbons (C_4-C_{27} *n*-alkanes and *n*-alk-1-enes), C_0-C_4 alkylphenols and C_0-C_2 alkylnaphthalenes. Ions used in quantitation are given in Table 7.

Ratio	Sample No.	
	Ringnes 139 (18)	Schei Point 29 (25)
Aliphatics/benzenes	3.35	3.25
Phenols/benzenes	0.49	0.14
Naphthalenes/benzenes	0.42	0.36

Fig. 1. (A) Location of oil and gas fields in arctic Canada. (B) Stratigraphic position of the Ringnes formation and Schei Point group, arctic islands, Canada (after Embry, 1991).

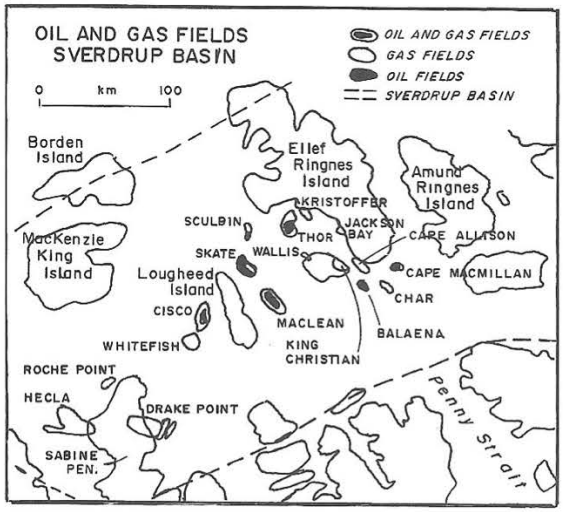

A

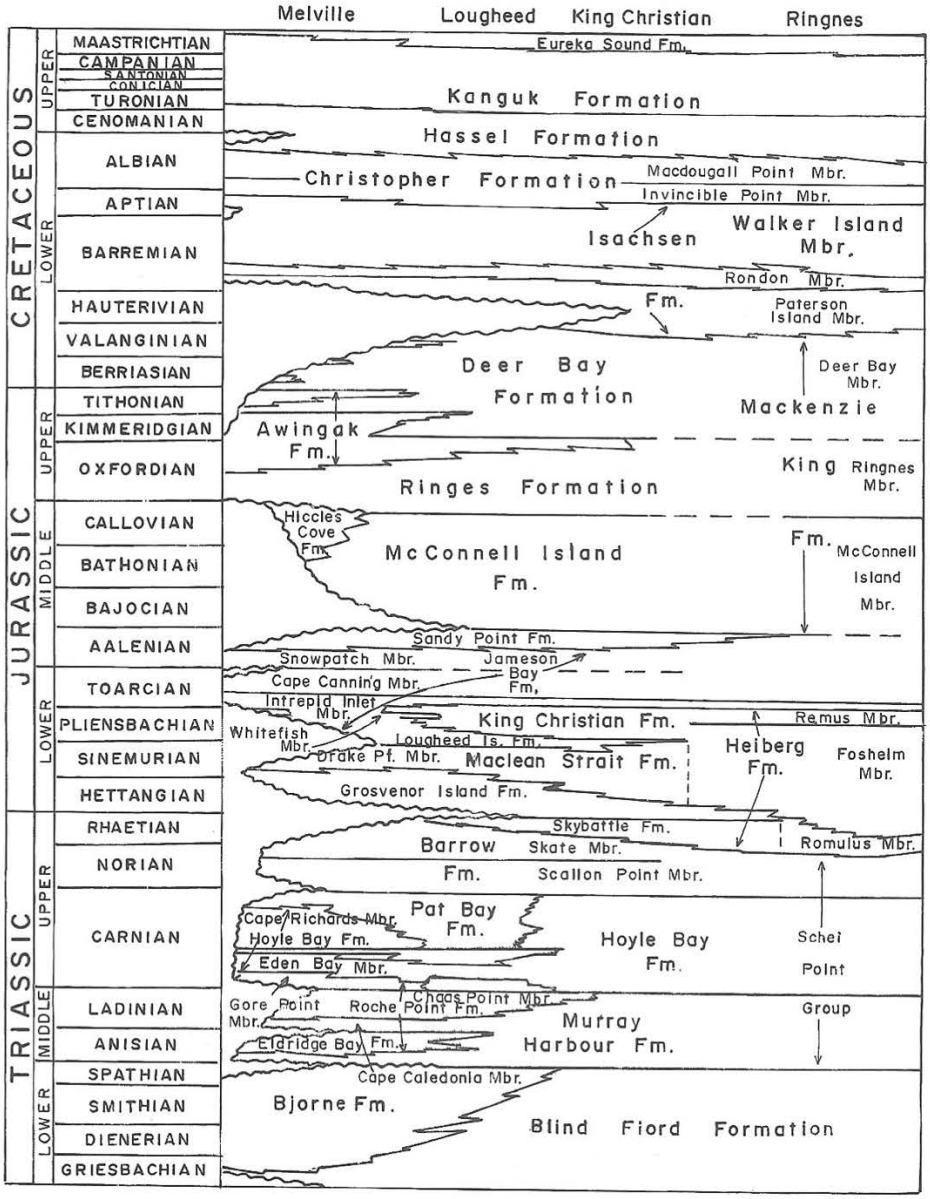

Fig. 2. Location map of samples from the Schei Point and Ringnes formation of arctic islands, Canada. Location number and well number. Schei Point group: 16 = Wilkens E-60; 20 = Jameson Bay; 29 = Satellite F-68; 44 = Drake Point F-16; 52 = Emerald K-33; 58 = Pollux G-60; 60 = Intrepid Inlet H-49; 64 = Sutherland 0 -23; 72 = Drake Point D-68; 73 = Andreasen L-32; 83 = Neil 0 -15; 94 = Sherard Bay F-14; 97 = Chads Creek B-64; 98 = Collingwood K-33; 100 = Pat Bay A-72; 133 = Roche Point J-43; 163 = Marryatt K-71; 166 = Grenadier A-26. Ringne s formation: 31 = Kristoffer Bay B-06; 35 = Dumbbells E-49; 41 = W. Amund I-44; 45 = Dome Bay P-36; 55 = Louise 0-25; 59 = Wallis K-62; 61 = E. Amund M-05; 86 = Elve M-40; 110 = Mocklin Point D-23; 118 = Jackson O-16A; 139 = Noice D-41; 157 = Hoodoo N-52; 161 = Sculpin K-08.

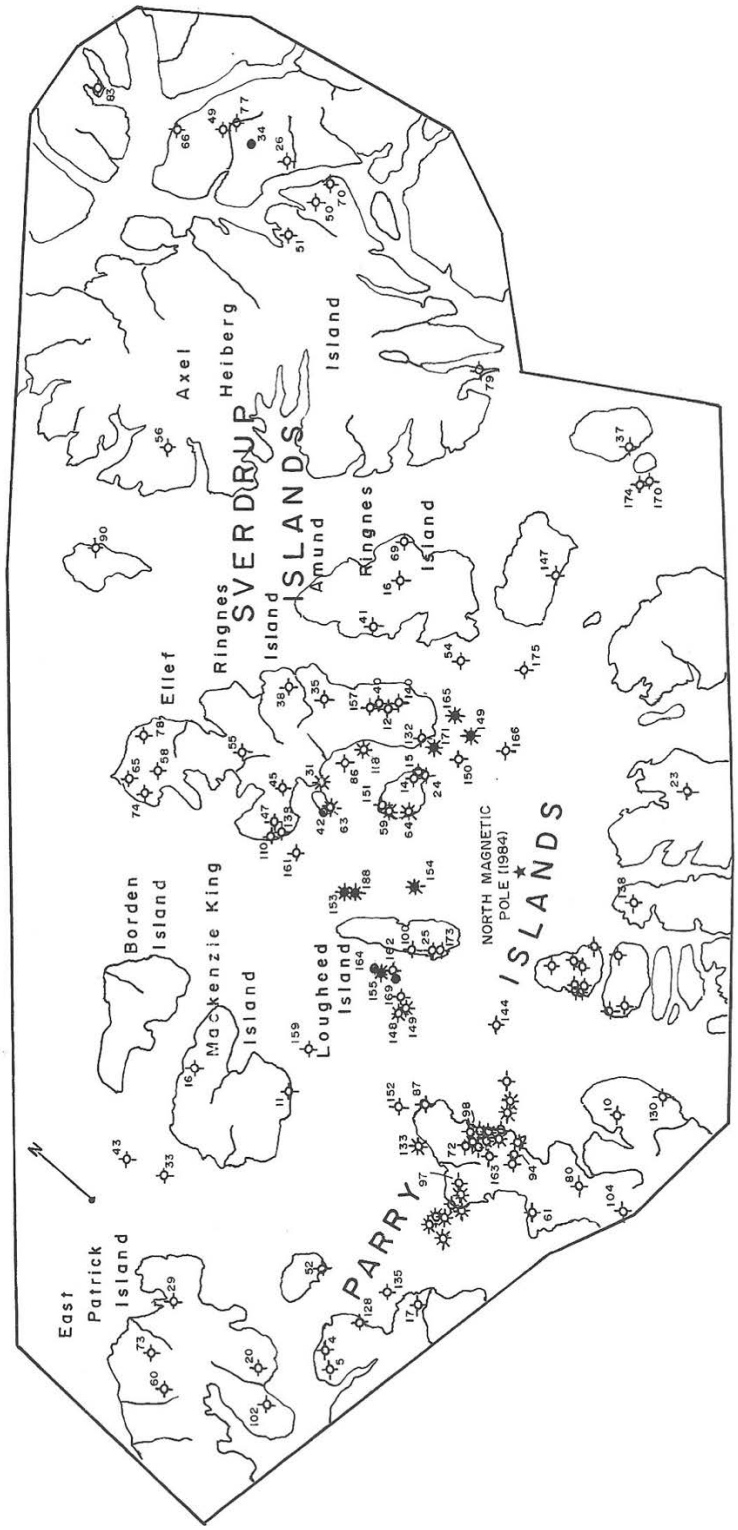

Fig. 3. Photomicrographs using kerogen smear slide and kerogen polished plug of Schei Point group of samples. (**A**) Sample (16) 32 using kerogen smear slide, blue incident light excitation, magnification X 250. Dinoflagellate (Dn), acritarch? (Ac), other alginite (telalginite; Al) and amorphous organic matter 1 (AOM1). (**B**) Sample (94) 27 using kerogen smear slide, blue incident light excitation, magnification X 250. Acritarch (Ac) and amorphous organic matter 2 (AOM2). (**C**) Sample (16) 32 using kerogen smear slide, blue incident light excitation, magnification X 250. Yellow and orange fluorescent amorphous organic matter l. (**D**) Sample (94) 27 using kerogen polished plug under blue light excitation, magnification X 50 0. Amorphous organic matter 2 (AOM2) and lamalginite (Al) with other liptodetrinite.

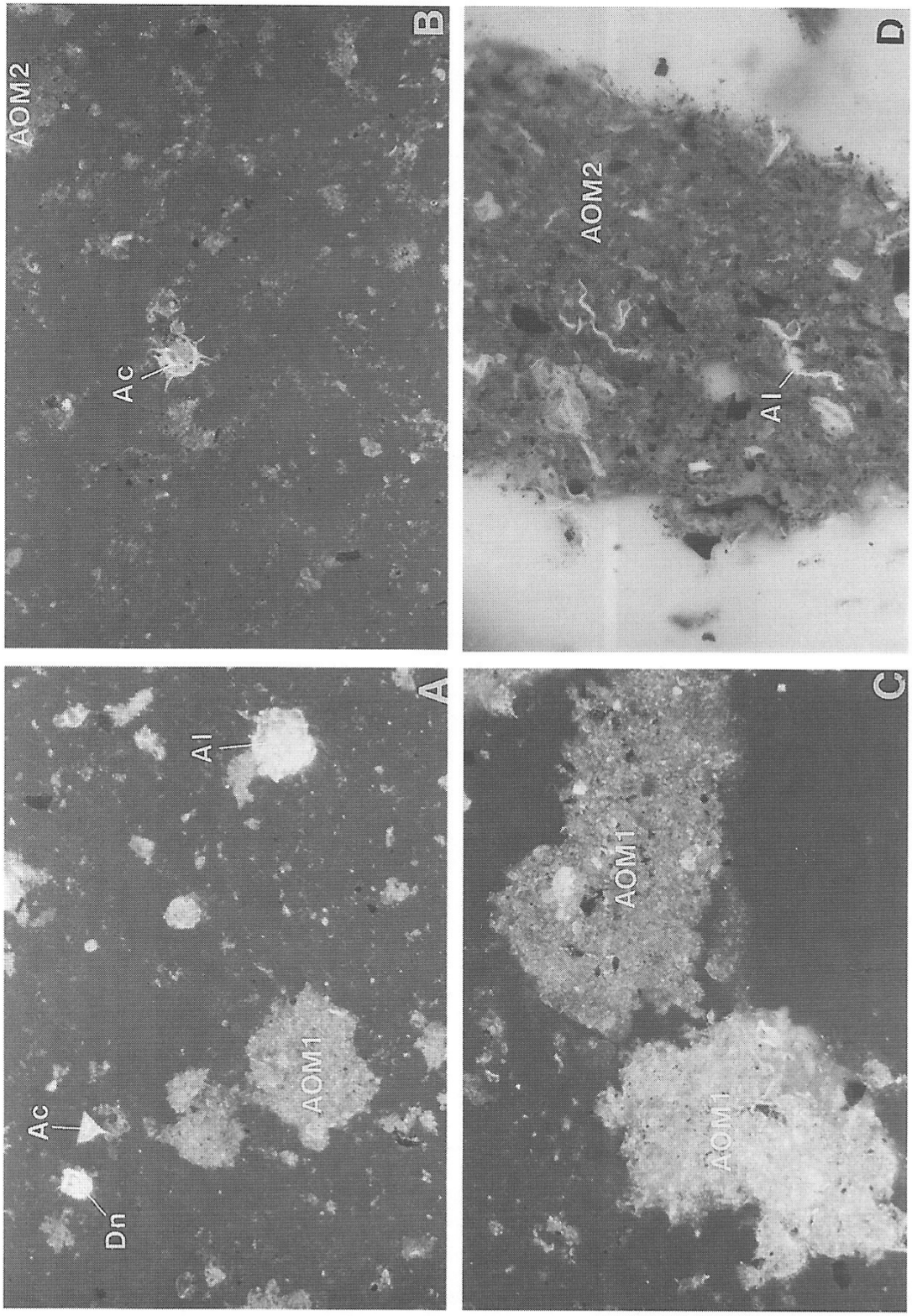

Fig. 4. Photomicrographs of kerogen polished plug of Ringnes and Schei Point samples under incident white light. (**A**) Sample (110) 24, Ringnes formation. Huminite (vitrinite) and unoxidized AOM2 with pyrite. (**B**) Sample (59) 33, Ringnes formation. huminite (vitrinite, recycled vitrinite, alginite (dark) and oxidized AOM2. (**C**) Sample (163) 19, Schei Point group. Vitrinite (autochthonous and recycled), AOM1 with internal reflection and pyrite. (**D**) Sample (83) 20, Schei Point group. Rank inertinite (micrinite and inertodetrinite) in AOM2 with vitrinite and pyrite.

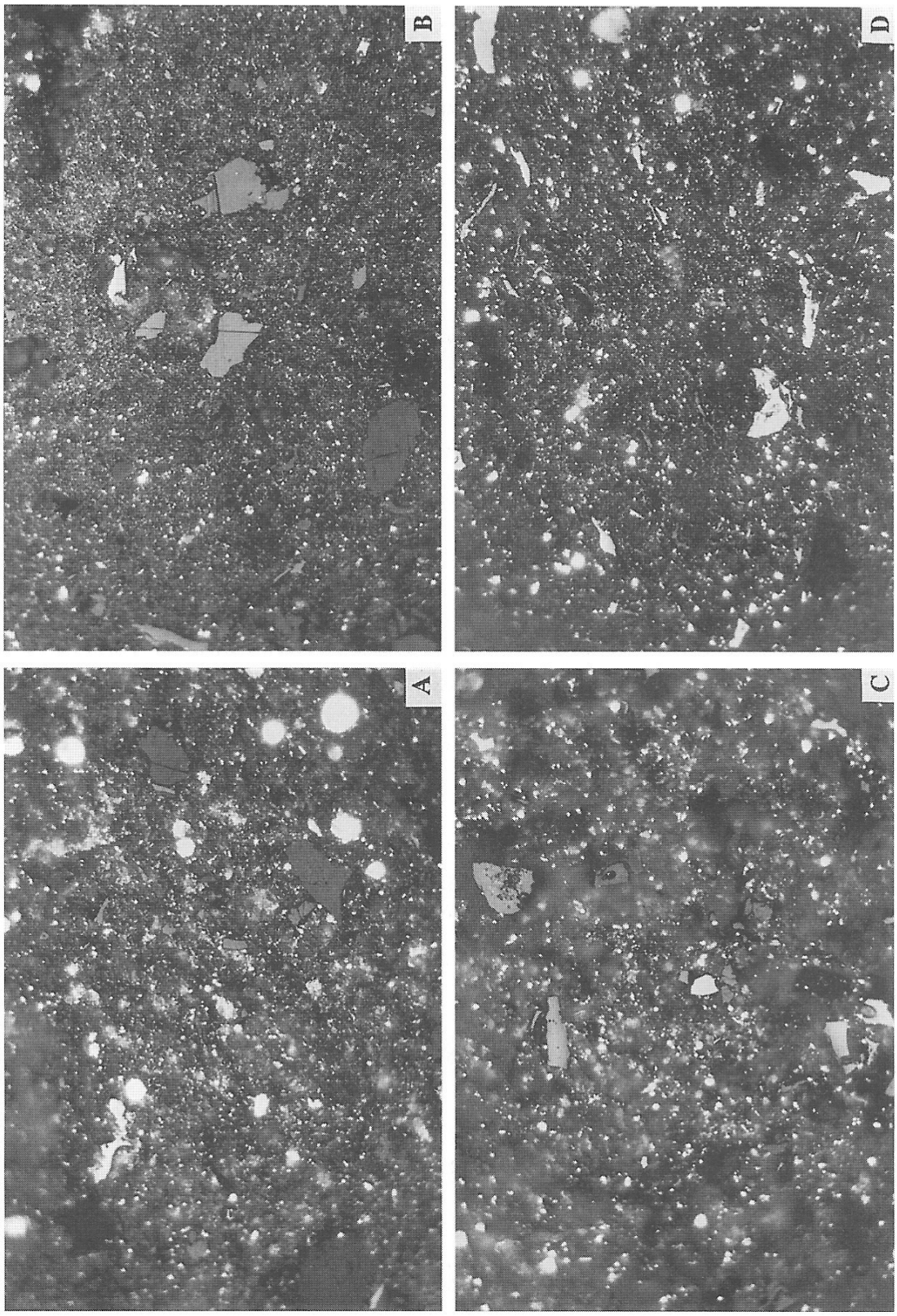

Fig. 5. A plot of vitrinite reflectance (% R_o) and hydrogen index (mg HC/g TOC) showing the maturation pathways of various kerogen types (after Mukhopadhyay, 1992b). The samples with an asterisk are of Ringnes formation and the samples with open squares are those from the Schei Point group.

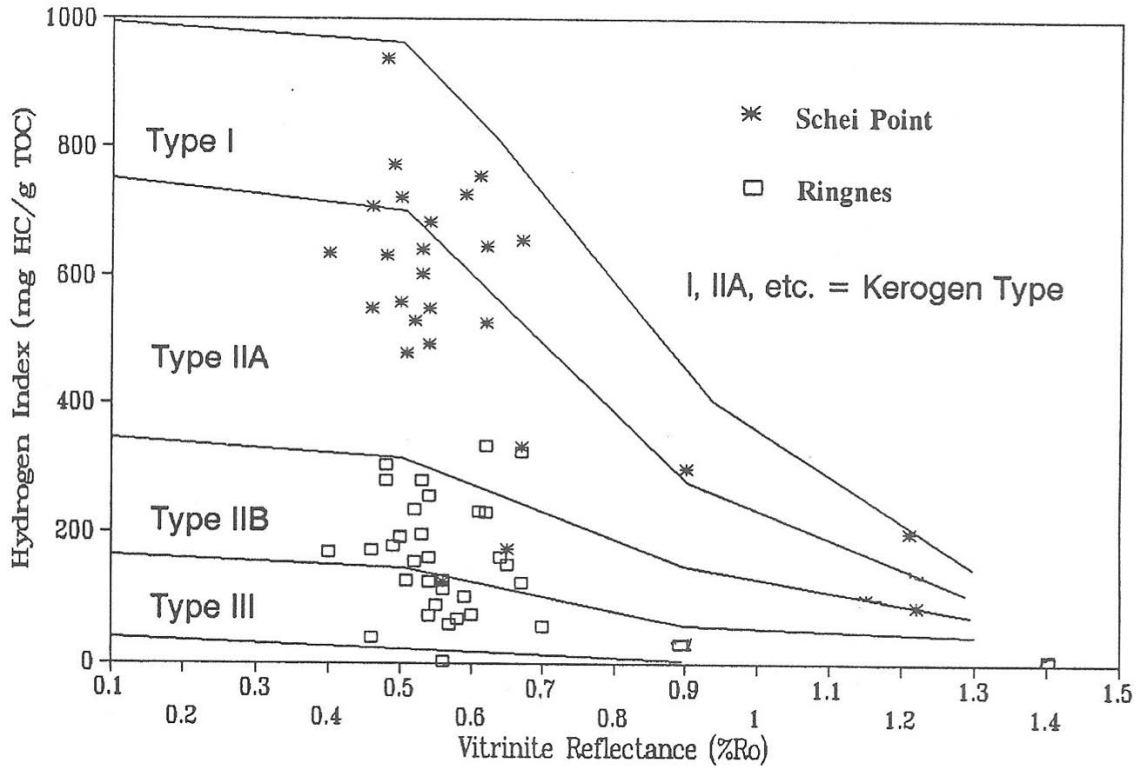

Fig. 6. A plot of total organic carbon (TOC in wt%) and bitumen content (mg extract/g TOC) using the samples from the Schei Point group (♦) and Ringnes formation (■).

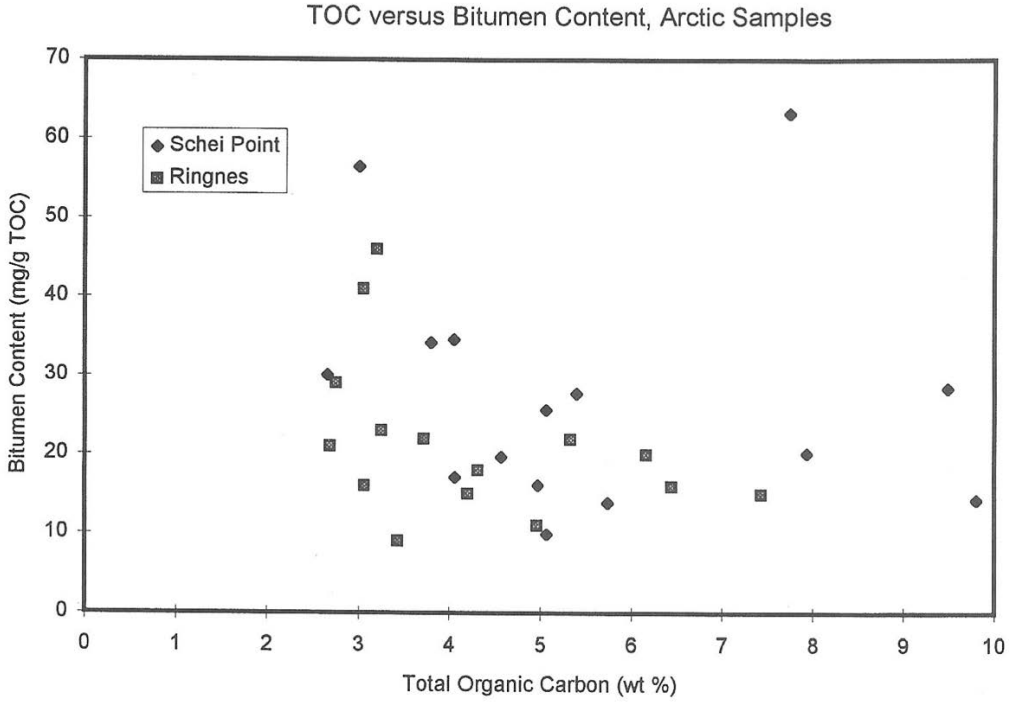

Fig. 7. Ternary diagram showing the composition of the extractable organic matter from the Ringnes formation and Schei Point group samples, based on separation by liquid chromatography.

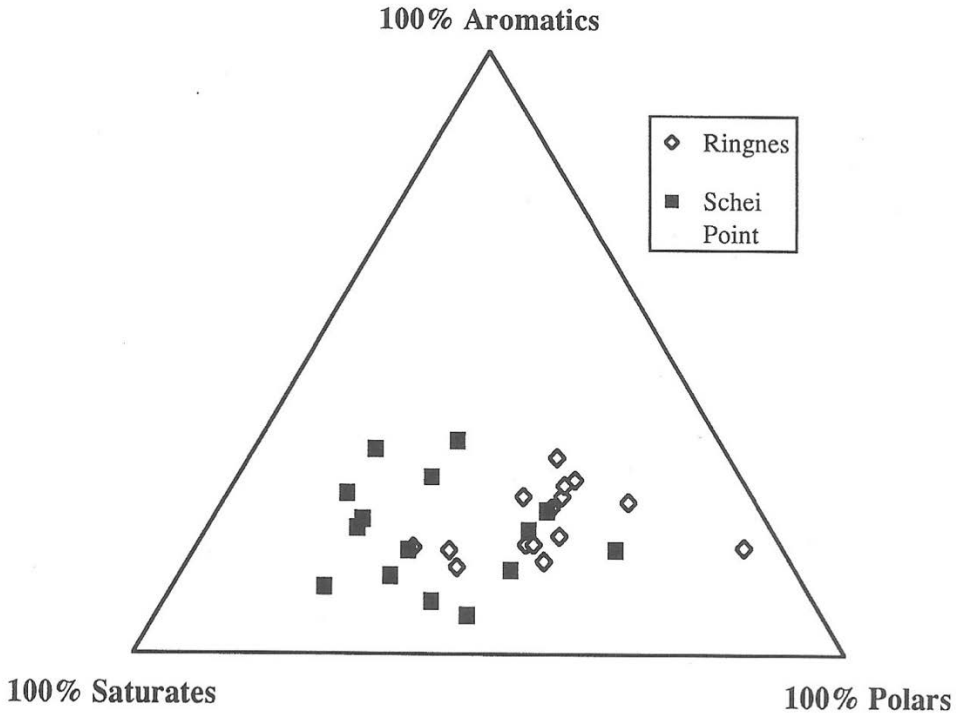

Fig. 8. Isoprenoid/normal alkane ratios (after Connan and Cassou, 1980) showing the position of Schei Point and Ringnes formation samples.

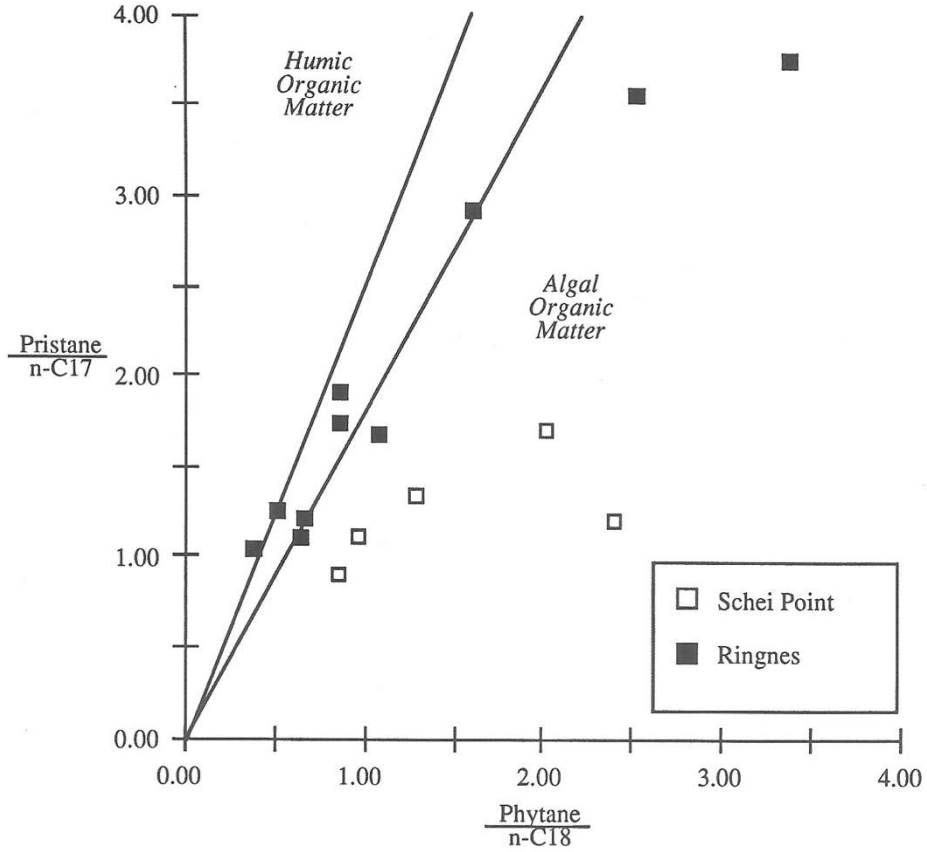

Fig. 9. Triterpane (m/z 191) mass fragmentograms. (A) Sample 60 (17), Intrepid Inlet H-49; B. Sample 133 (23), Roche Point J-43, Schei Point group. For identification see Table 4.

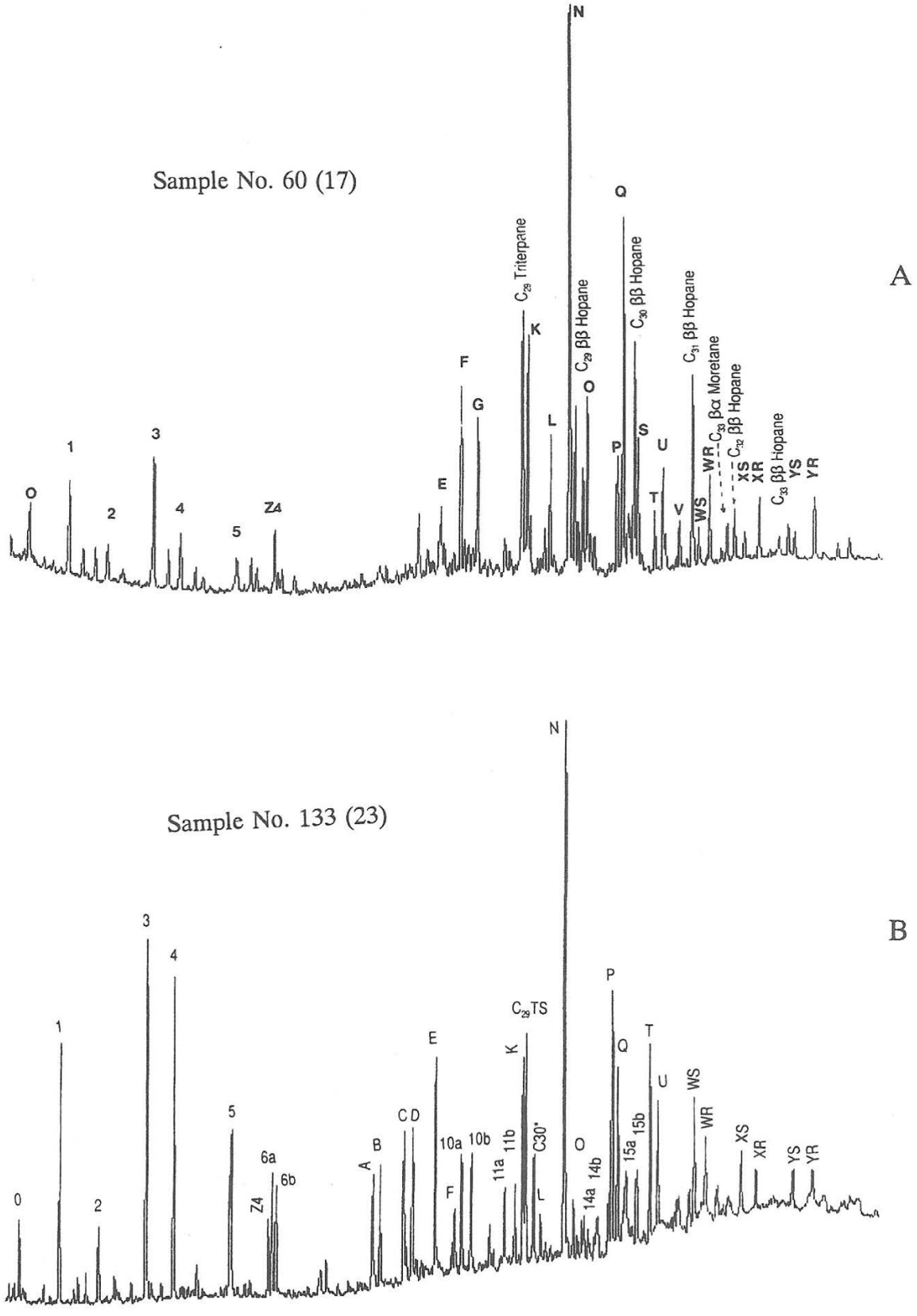

Fig. 10. Triterpane (m/z 191) mass fragmentograms. (A) Sample 161 (20), Sculpin K-08. (B) Sample 45.(7), Dome Bay P-36; Ringnes formation. For identification see Table 4.

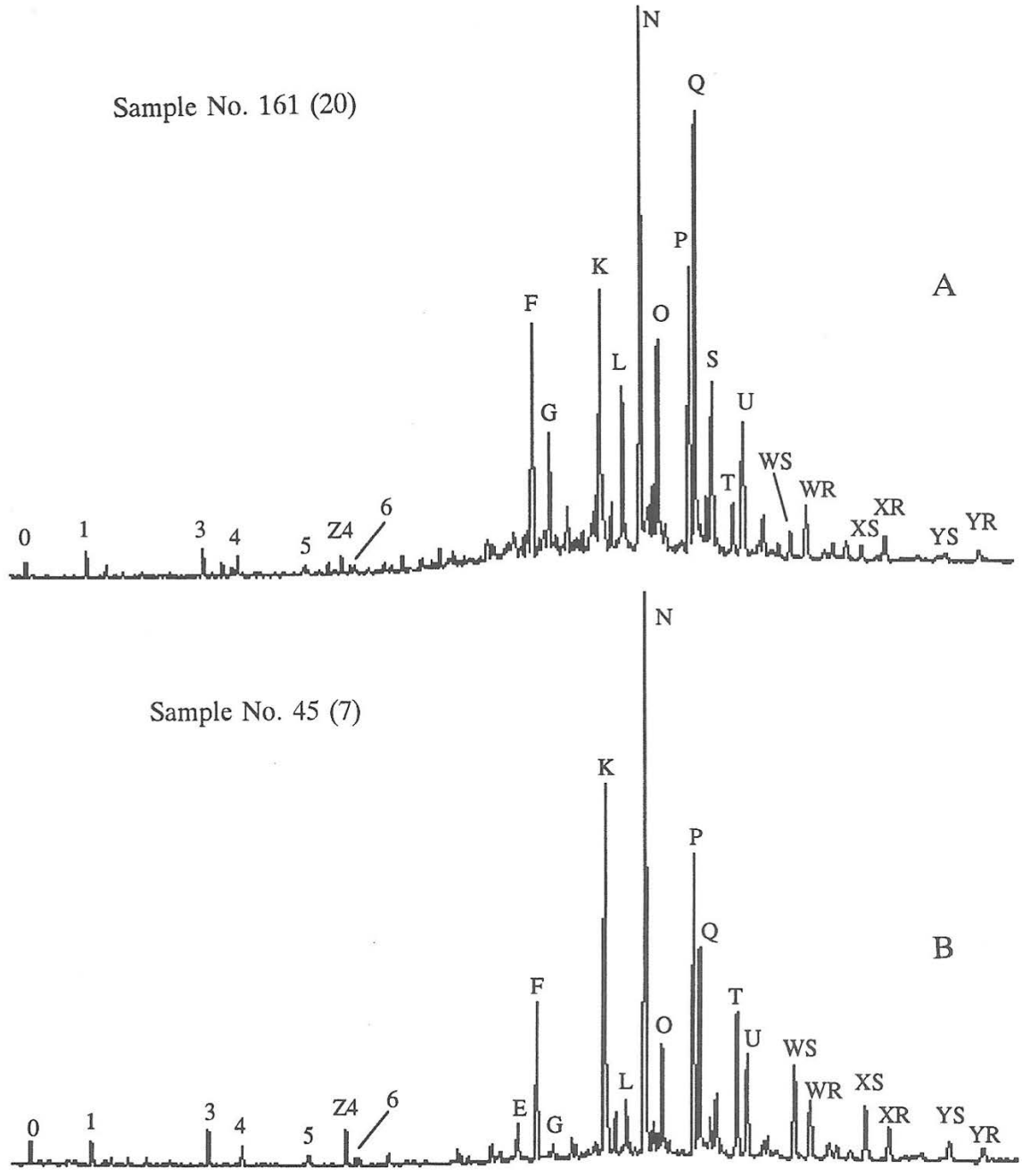

Fig. 11. Sterane (m/z 217) mass fragmentograms. (A) Sample 60 (17), Intrepid inlet H-49. (B) Sample 133 (23), Rache Point J-43, Schei Point group. For identification see Table 5.

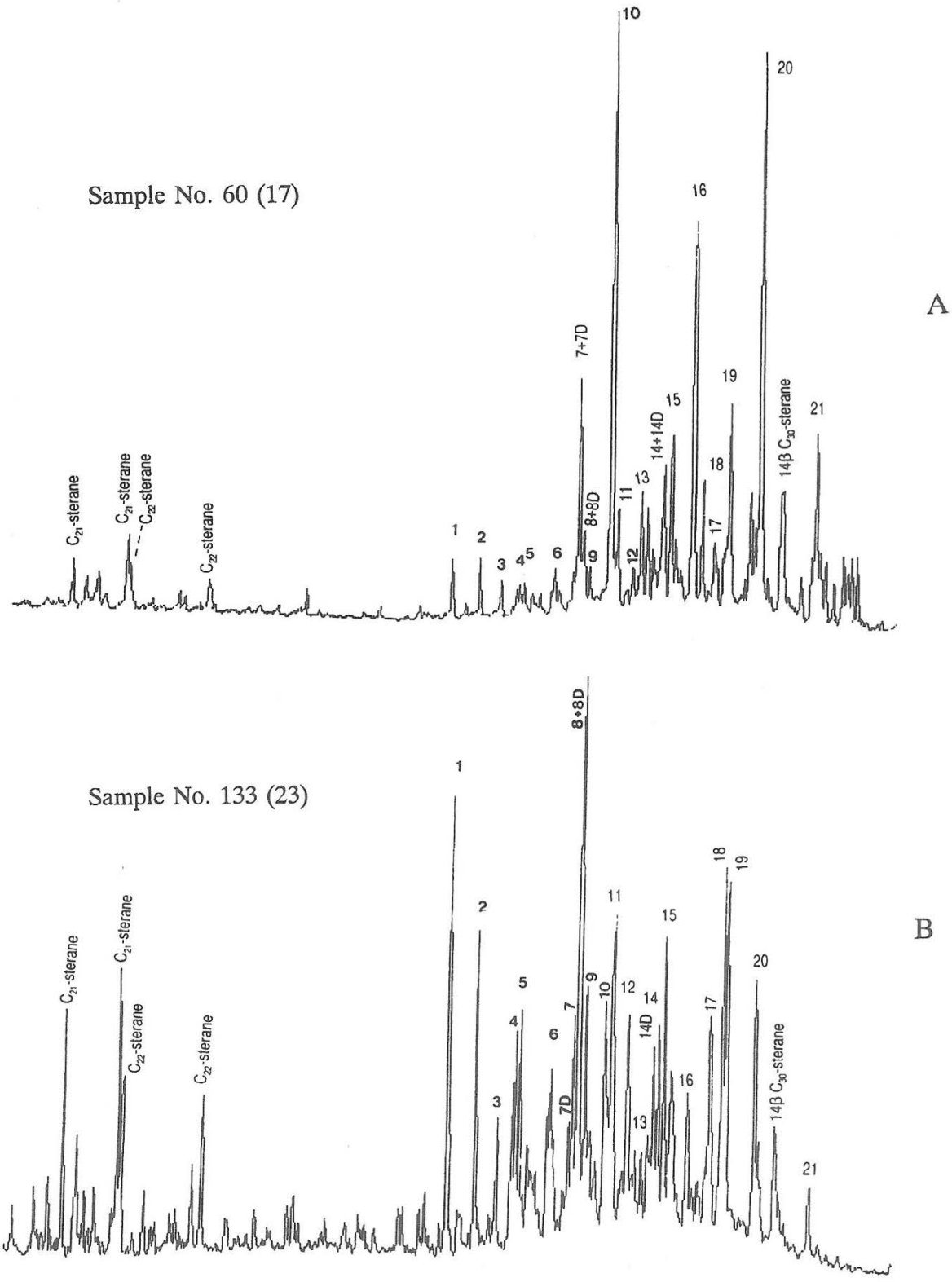

Fig. 12. Sterane (m/z 217) mass fragmentograms. (A) sample 161 (20), Sculpin K-08. (B) Sample (45) 7, Dome Bay P-36; Ringnes formation. For identification see Table 5.

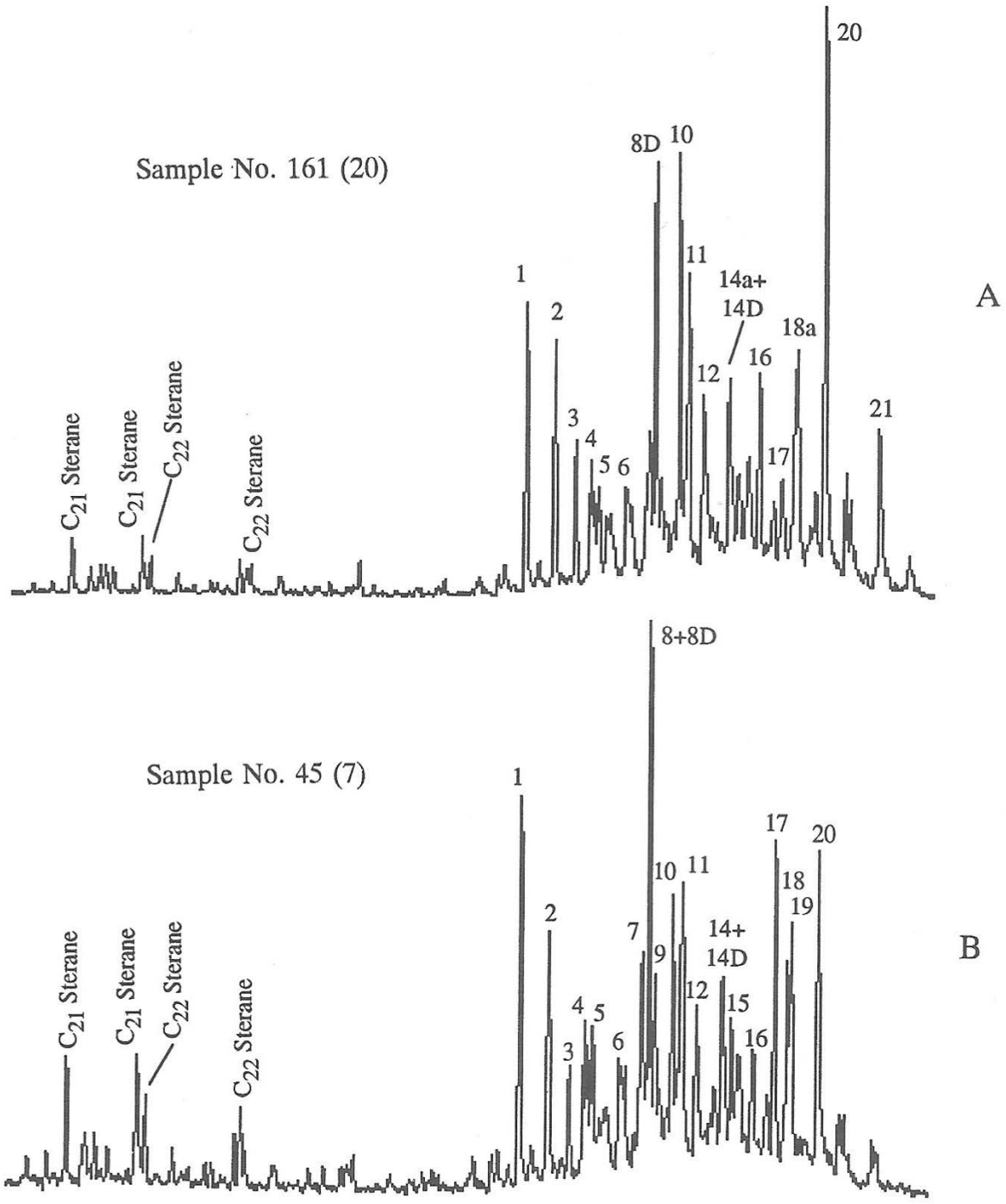

Fig . 13. Ternary diagram showing relative percentages of C_{27}, C_{28} and C_{29} $\alpha\alpha\alpha$ 20R steranes for the Ringnes formation and Schei Point group extracts. Quantitations performed on m/z 217 mass fragmentograms.

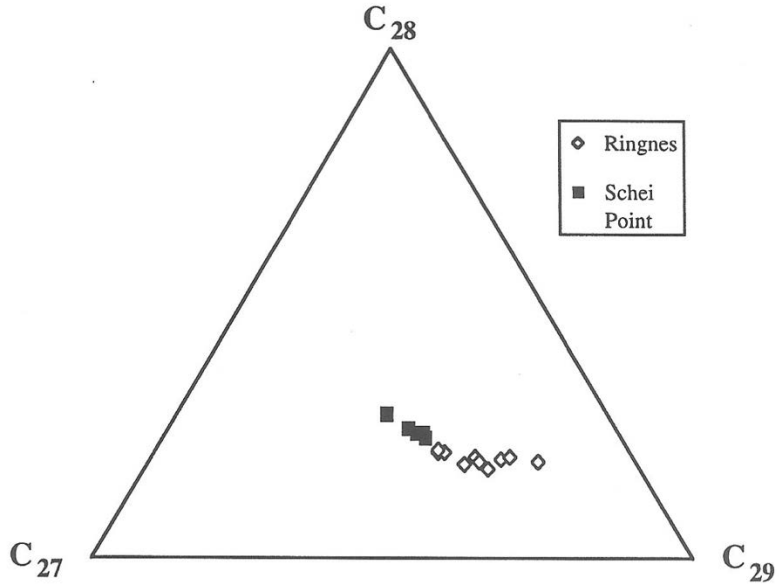

Fig. 14. (A) Ratio of C_{27} to C_{29} $\alpha\alpha\alpha$ 20R steranes as a function of the ratio of alginite +AOM1 + AOM2 to vitrinite. (B) Ratio of diasteranes to regular steranes as a function of the ratio of alginite +AOM1 +AOM2 to vitrinite. Maceral percentages determined petrographically. Sterane quantitations performed on m/z 217 mass fragmentograms.

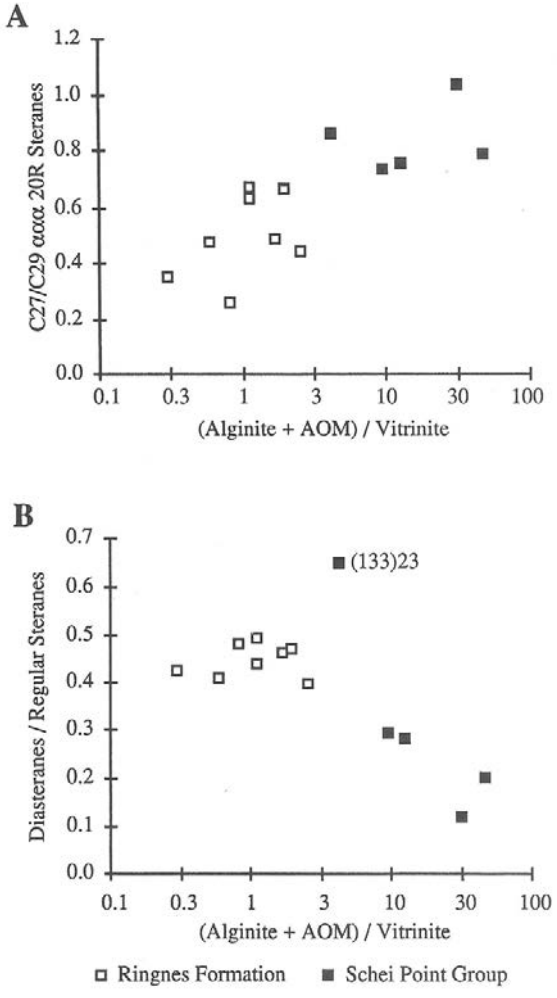

Fig. 15. A plot of stable carbon isotope values of saturate and aromatics fraction of the extract. The line is drawn after Sofer (1984).

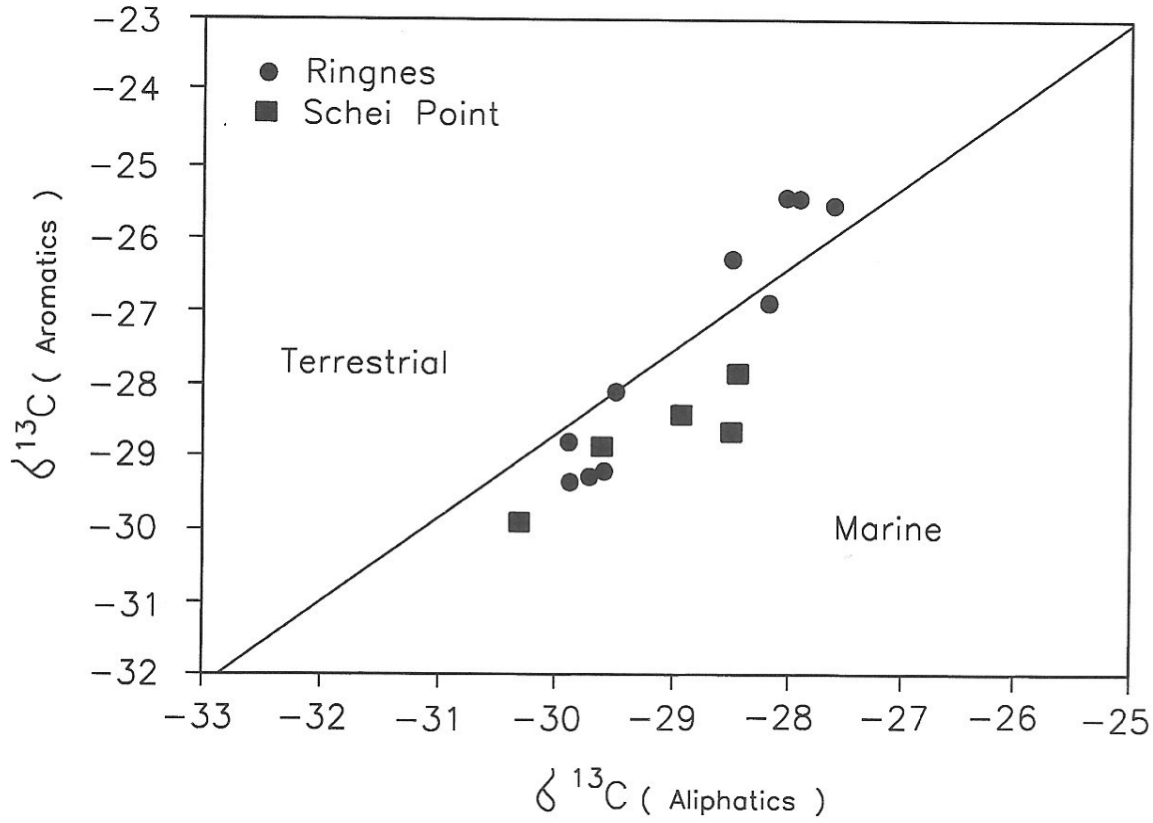

Fig. 16. Pyrolysis-GC/ MS total ion chromatograms of the 610°C flash pyrolyzates of two shale samples 29 (25) for the Schei Point group and 139 (18) for the Ringnes formation.